Inorganic Chemistry

Article

pubs.acs.org/IC

Scrutinizing Low-Spin Cr(II) Complexes

Christopher C. Scarborough,*[,†,‡] Stephen Sproules,[∥] Christian J. Doonan,[§] Karl S. Hagen,[‡] Thomas Weyhermüller,[†] and Karl Wieghardt*[,†]

[†]Max-Planck-Institut für Bioanorganische Chemie, Stiftstraße 34-36, D-45470 Mülheim an der Ruhr, Germany

[‡]Department of Chemistry, Emory University, 1515 Dickey Drive, Atlanta Georgia 30322, United States

[∥]EPSRC National UK EPR Facility and Service, Photon Science Institute, The University of Manchester, Oxford Road, Manchester M13 9PL, U.K.

[§]School of Chemistry and Physics, The University of Adelaide, SA 5005, Australia

Supporting Information

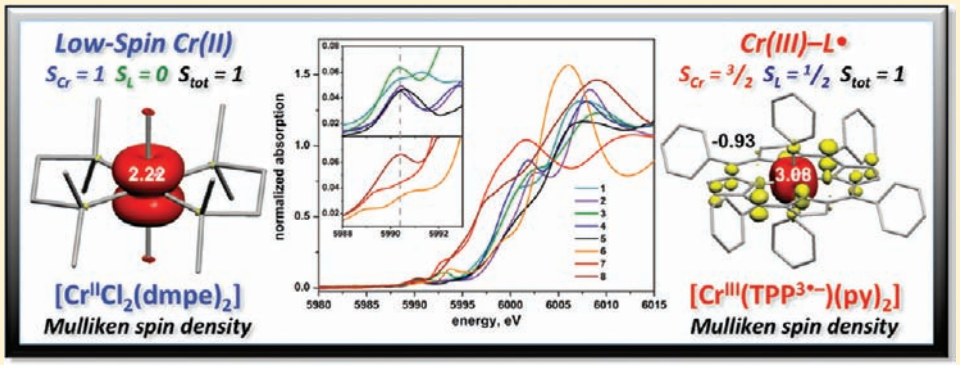

ABSTRACT: The oxidation state of the chromium center in the following compounds has been probed using a combination of chromium K-edge X-ray absorption spectroscopy and density functional theory: $[Cr(phen)_3][PF_6]_2$ (**1**), $[Cr(phen)_3][PF_6]_3$ (**2**), $[CrCl_2(^tbpy)_2]$ (**3**), $[CrCl_2(bpy)_2]Cl_{0.38}[PF_6]_{0.62}$ (**4**), $[Cr(TPP)(py)_2]$ (**5**), $[Cr(^tBuNC)_6][PF_6]_2$ (**6**), $[CrCl_2(dmpe)_2]$ (**7**), and $[Cr(Cp)_2]$ (**8**), where phen is 1,10-phenanthroline, ^{t}bpy is 4,4′-di-*tert*-butyl-2,2′-bipyridine, and TPP^{2-} is doubly deprotonated 5,10,15,20-tetraphenylporphyrin. The X-ray crystal structures of complexes **1**, $[Cr(phen)_3][OTf]_2$ (**1′**), and **3** are reported. The X-ray absorption and computational data reveal that complexes **1**−**5** all contain a central Cr(III) ion ($S_{Cr} = {}^3/_2$), whereas complexes **6**−**8** contain a central low-spin ($S = 1$) Cr(II) ion. Therefore, the electronic structures of **1**−**8** are best described as $[Cr^{III}(phen^•)(phen^0)_2][PF_6]_2$, $[Cr^{III}(phen^0)_3][PF_6]_3$, $[Cr^{III}Cl_2(^tbpy^•)(^tbpy^0)]$, $[Cr^{III}Cl_2(bpy^0)_2]Cl_{0.38}[PF_6]_{0.62}$, $[Cr^{III}(TPP^{3•-})(py)_2]$, $[Cr^{II}(^tBuNC)_6][PF_6]_2$, $[Cr^{II}Cl_2(dmpe)_2]$, and $[Cr^{II}(Cp)_2]$, respectively, where (L^0) and $(L^•)^-$ (L = phen, ^{t}bpy, or bpy) are the diamagnetic neutral and one-electron-reduced radical monoanionic forms of L, and $TPP^{3•-}$ is the one-electron-reduced doublet form of diamagnetic TPP^{2-}. Following our previous results that have shown $[Cr(^tbpy)_3]^{2+}$ and $[Cr(tpy)_2]^{2+}$ (tpy = 2,2′:6′,2″-terpyridine) to contain a central Cr(III) ion, the current results further refine the scope of compounds that may be described as low-spin Cr(II) and reveal that this is a very rare oxidation state accessible only with ligands in the strong-field extreme of the spectrochemical series.

INTRODUCTION

The oxidation-state formalism is pervasive in inorganic and organometallic chemistry and is a core concept in chemists' vernacular for classifying compounds and describing their reactivity.[1] A working knowledge of synthetically accessible oxidation states for each transition metal is critical for predicting stability of new compounds and the viability of proposed intermediates. Beyond being a simple formalism, oxidation states may be scrutinized spectroscopically, although spectroscopic (physical) and formal oxidation states are not always congruous.[2] If cumulated experimental data reveal mounting disagreement between formal and spectroscopic oxidation state for a given formal-oxidation-state/spin-state combination, the accessibility of such species should be called into question.

Mounting data published from our laboratory has revealed that low-spin Cr(II) (d^4, $S = 1$)[3] may be a formal oxidation state that has been invoked incorrectly in many cases, and these data have caused us to question the stability of low-spin Cr(II) in general.[4] Inorganic texts discussing low-spin Cr(II) compounds identify up to five examples:[5] (1) $[Cr(CN)_6]^{4-}$, (2) $[Cr(bpy/phen)_3]^{2+}$, (3) $[Cr(tpy)_2]^{2+}$, (4) $[CrX_2(bpy/phen)_2]$, and (5) $[CrX_2(L—L)_2]$, where L—L is a diphosphine or diarsine bidentate ligand; other formally low-spin Cr(II)

Received: April 30, 2012
Published: June 7, 2012

   dx.doi.org/10.1021/ic300882r | *Inorg. Chem.* 2012, 51, 6969−6982

compounds have been reported as well.[6] In a recent series of papers,[4] we have demonstrated that $[Cr(^tbpy)_3]^{2+}$ and $[Cr(tpy)_2]^{2+}$, both $S = 1$ compounds, have been incorrectly assigned as containing Cr(II): spectroscopic and theoretical studies reveal that the chromium ion is in the +III oxidation state. The electron previously assigned to the metal in these cases resides in a ligand-centered orbital and is antiferromagnetically coupled to the high-spin Cr(III) center ($S_{Cr} = {}^3/_2$) to afford the observed triplet ground spin state. On the other hand, we demonstrated that $K_4[Cr(CN)_6]$[7] is indeed best described as containing low-spin Cr(II), which is unsurprising given the π-accepting character of the strong-field cyanide ligands and the lack of available low-energy ligand-centered orbitals.[8] In fact, comparison of low-valent bpy, phen, tpy, and cyanide compounds have led some authors to identify bpy, phen, and tpy as strong-field ligands because of their ability to stabilize low-valent species analogously to the strong-field cyanide ligand.[5,9] However, spectroscopic studies had already demonstrated that bpy and phen are only very weak π-acceptor ligands.[10] In fact, Josephsen and Schäffer note that, for homoleptic octahedral Cr(III), bpy and phen are *weaker-field* ligands than ethylene diamine![10b] The confusion arising from these inconsistencies clearly has its origins in misleading formal oxidation state assignments.

The observation that low-spin Cr(II) complexes may be rarer than previously believed led us to undertake a more general study of compounds described in the literature as containing low-spin Cr(II), the results of which are presented in this manuscript. We have identified the following compounds as representative examples of "low-spin Cr(II)" species: $[Cr(phen)_3][PF_6]_2$ (**1**), $[CrCl_2(^tbpy)_2]$ (**3**), $[Cr(TPP)(py)_2]$ (**5**),[6b,11] $[Cr(^tBuNC)_6][PF_6]_2$ (**6**),[6d] $[CrCl_2(dmpe)_2]$ (**7**),[12] and $[Cr(Cp)_2]$ (**8**)[6a,j] (Chart 1). We have investigated the

Chart 1. Complexes and Ligand Abbreviations Used

$[Cr(phen)_3][PF_6]_2$	**1**
$[Cr(phen)_3][OTf]_2$	**1'**
$[Cr(phen)_3][PF_6]_3$	**2**
$[CrCl_2(^tbpy)_2]$	**3**
$[CrCl_2(bpy)_2][PF_6]_{0.62}Cl_{0.38}$	**4**
$[Cr(TPP)(py)_2]$	**5**
$[Cr(^tBuNC)_6][PF_6]_2$	**6**
$[CrCl_2(dmpe)_2]$	**7**
$[Cr(Cp)_2]$	**8**

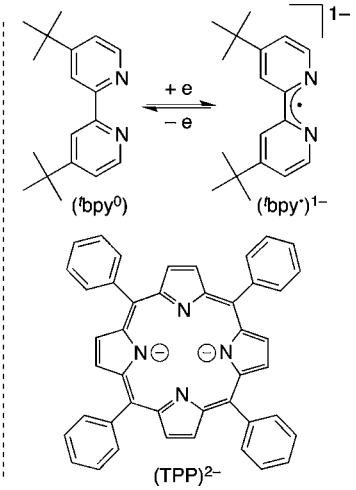

spectroscopic (physical) oxidation state of the chromium center in each compound using Cr K-edge X-ray absorption spectroscopy and have examined each compound using (broken-symmetry) density functional theory. The results of these studies are summarized as follows:

(1) Of the compounds examined, only **6**–**8** are correctly described as containing a low-spin Cr(II) ion.

(2) **1**, **3**, and **5** all contain a central Cr(III) ion ($S_{Cr} = {}^3/_2$), where the excess electron is localized in phen-, ^{t}bpy-, and TPP-centered orbitals, respectively, and is antiferromagnetically coupled to the Cr(III) ion to yield the observed triplet ground spin state.

(3) **3** contains a ligand-centered radical that is *localized* on a single ^{t}bpy ligand in the solid state (Robin-Day[13] Class I ligand mixed valency) and is best described as $[Cr^{III}Cl_2(^tbpy^{\bullet})(^tbpy^0)]$, where $(^tbpy^0)$ and $(^tbpy^{\bullet})^-$ are the diamagnetic neutral and doublet monoanionic forms of 4,4′-di-*tert*-butyl-2,2′-bipyridine, respectively. On the other hand, the extent of delocalization of the phen-centered radical in **1** and $[Cr(phen)_3][OTf]_2$ (**1′**) is somewhat ambiguous, although the data are suggestive of a more *delocalized* radical (Class II, II/III,[14] or III ligand mixed valency) in **1** and **1′** than is observed in **3**.

Our results allow us to make the following conclusions concerning low-spin Cr(II):

(1) Low-spin Cr(II) is a very uncommon oxidation state and is stabilized only by ligands in the strong-field extreme of the spectrochemical series, including phosphine,[6g,h,m,n,12b−j] arsine,[12a] cyanide,[7] isonitrile,[6d] pentadienide,[6l−n] allyl,[6n] aryl,[6o] and cyclopentadienide.[6a,g,h,j−l,o]

(2) Chromium compounds bearing ligands with energetically low-lying lowest unoccupied molecular orbitals (LUMOs) (e.g., bpy, phen, tpy, and TPP^{2-}) that are formally low-spin Cr(II) compounds are very likely better described as Cr(III) species that are antiferromagnetically coupled to a ligand-centered radical.

With these studies, we demonstrate that the oxidation-state formalism may be misleading for compounds formally described as low-spin Cr(II). This already rare oxidation state is in fact even rarer than previously believed,[5] comprising only three types of compounds: (1) organometallic species (containing cyclopentadienide,[6a,g,h,j−l,o] pentadienide,[6l−n] allyl,[6n] and/or aryl[6o] ligands), (2) $[Cr^{II}X_2(R_3Z)_4]$,[12] and (3) $[Cr^{II}(CNR')_6]^q$ [Z = P, As; X = halide, CN^-, amido, or alkyl; R′ = alkyl or aryl ($q = 2+$)[6d] or lone pair ($q = 4-$)[7]].

EXPERIMENTAL SECTION

1.1. General Considerations. The following syntheses were carried out using standard Schlenk-line procedures or a glovebox in the absence of dioxygen and water using rigorously dried solvents. The complexes $[CrCl_2(bpy)_2][PF_6]_{0.62}Cl_{0.38}$ (**4**),[15] $[Cr(TPP)(py)_2]$ (**5**),[6b,11] $[Cr(^tBuNC)_6][PF_6]_2$ (**6**),[6d] and $[CrCl_2(dmpe)_2]$ (**7**)[12c] were prepared as described in the literature. $[Cr(Cp)_2]$ (**8**)[6a,j] was purchased from Strem and used as received.

1.2. Physical Measurements. Electronic spectra of complexes were recorded with a Perkin-Elmer Lambda 19 double-beam spectrophotometer (200−2100 nm). Variable temperature (4−300 K) magnetization data were recorded in a 1 T magnetic field on a SQUID magnetometer (MPMS Quantum Design). The experimental magnetic susceptibility data were corrected for underlying diamagnetism using tabulated Pascal's constants. Elemental analyses were performed by H. Kolbe at the Mikroanalytischen Labor in Mülheim an der Ruhr, Germany.

1.3. Synthesis of Compounds. *$[Cr(phen)_3][PF_6]_2$ (1).* phen·H_2O (2.425 g, 12.2 mmol), $CrCl_2$ (505 mg, 4.1 mmol), and 30 mL of degassed water were combined under argon in a 50 mL Schlenk flask. The solution was stirred at room temperature for 20 h, during which time the color changed from light blue to deep dark green. Five milliliters of a 1.6 M solution of NH_4PF_6 (8.0 mmol) in degassed water was added to the reaction mixture, resulting in the precipitation of $[Cr(phen)_3][PF_6]_2$. The suspension was filtered through a Schlenk frit, and the solid was washed with 50 mL of degassed water. The solid was dried under vacuum, taken up in dry MeCN, and filtered. Removal of the MeCN under vacuum afforded 3.01 g of $[Cr(phen)_3][PF_6]_2$

dx.doi.org/10.1021/ic300882r | Inorg. Chem. 2012, 51, 6969−6982

Table 1. Crystallographic Data for 1, 1′, and 3

	1·2.5CH_3CN	1′	3
chem. formula	$C_{41}H_{31.5}CrF_{12}N_{8.5}P_2$	$C_{38}H_{24}CrF_6N_6O_6S_2$	$C_{36}H_{48}Cl_2CrN_4$[a]
Fw	985.19	890.75	659.68
space group	$R\bar{3}$, No. 148	$P\bar{1}$, No. 2	$P2_1/c$, No. 14
a, Å	14.9676(11)	9.4602(8)	25.027(5)
b, Å	14.9676(11)	13.5845(11)	11.599(2)
c, Å	63.056(4)	14.9225(13)	53.487(9)
α, deg	90	96.019(2)	90
β, deg	90	103.230(2)	90.375(3)
γ, deg	120	102.314(2)	90
V, Å^3	12233.8(15)	1799.9(3)	15526(5)
Z	12	2	16
T, K	100(2)	100(2)	100(2)
r calcd, g cm^{-3}	1.605	1.644	1.129[a]
refl. collected/$2\Theta_{max}$	29308/55.00	21151/60.0	253579/50.00
unique refl./$I > 2\sigma(I)$	6265/4939	10416/8366	27334/21283
no. of params/restr.	402/12	569/0	1694/102
l, Å /m (Ka), cm^{-1}	0.71073/4.59	0.71073/5.2	0.71073/4.59[a]
R1[b]/goodness of fit[c]	0.1069/1.133	0.054/1.05	0.0648/1.105
wR2[d] ($I > 2\sigma(I)$)	0.2315	0.137	0.1284
residual density, e Å^{-3}	+0.78/−1.47	+1.50/−0.48	+0.65/−0.66
CCDC depository code	878595	878597	878596

[a]Disordered solvent (thf) has been removed using the program Platon/Squeeze.[19] [b]Observation criterion: $I > 2\sigma(I)$. R1 = $\sum||F_o| - |F_c||/\sum|F_o|$. [c]GoF = $[\sum[w(F_o^2 - F_c^2)^2]/(n-p)]^{1/2}$. [d]wR2 = $[\sum[w(F_o^2 - F_o^2)^2]/\sum[w(F_o^2)^2]]^{1/2}$, where $w = 1/\sigma^2(F_o^2) + (aP)^2 + bP$, $P = (F_o^2 + 2F_c^2)/3$.

(83% yield). X-ray-quality crystals were grown by vapor diffusion of Et_2O onto a concentrated solution of **1** in MeCN. Anal. Calc. for $C_{36}H_{24}N_6CrP_2F_{12}$: C, 48.99; H, 2.74; N, 9.52; Cr, 5.89; P, 7.02. Found: C, 48.86; H, 2.67; N, 9.49; Cr, 5.79; P, 6.95.

[Cr(phen)$_3$](OTf)$_2$ (1′). Three equivalents of 1,10′-phenanothroline (0.3 mmol, 55 mg) were dissolved in 0.5 mL of acetonitrile, and were mixed with a 0.5 mL acetonitrile solution of Cr(OTf)$_2$·2MeCN (0.1 mmol, 43.5 mg).[49] The resulting green-brown solution produced dark green crystals after diffusion of diethyl ether into the mixture for 2 days (72 mg, 81% yield). M/z^+: 560.0 obs., 560.5 calc. $\{Cr(phen)_2(OTf)\}^+$, μ_{eff}(298 K) = 3.28 μ_B.

[Cr(phen)$_3$][PF$_6$]$_3$ (2). $[Cr(phen)_3][PF_6]_2$ (100 mg, 0.11 mmol) was dissolved in 2 mL of MeCN. Separately, $AgPF_6$ (30 mg, 0.12 mmol) was dissolved in 1 mL of MeCN, and this solution was added over 30 s to the stirred $[Cr(phen)_3][PF_6]_2$ solution, resulting in a brown suspension. After stirring for 15 min, the MeCN was removed under vacuum to afford a brown residue. Tetrahydrofuran (THF) was added to the resulting residue, which was scraped to a powder with a spatula. The THF was decanted, and the residue was washed again with THF. Dissolution of the orange residue in MeCN, filtration through Celite, and solvent removal under vacuum afforded pure, air-stable, yellow-orange $[Cr(phen)_3][PF_6]_3$ in 70% yield (82 mg). This material may be crystallized by vapor diffusion of Et_2O onto a concentrated solution in MeCN. Anal. Calc. for $C_{36}H_{24}N_6CrP_3F_{18}$: C, 42.08; H, 2.35; N, 8.18; Cr, 5.06; P, 9.04. Found: C, 41.95; H, 2.72; N, 8.40; Cr, 5.18; P, 9.20.

[CrCl$_2$(^{t}bpy)$_2$] (3). Anhydrous $CrCl_2$ (23 mg, 0.19 mmol) and ^{t}bpy (101 mg, 0.38 mmol) were combined in 3 mL of dry THF. Within seconds, a deep purple color developed. After stirring for 1 h the mixture was filtered through Celite and the solvent was removed under vacuum. After scraping the residue to a powder with a spatula and drying it under high vacuum for 4 h, the powder was redissolved in toluene to afford a deep blue-green solution. Filtration of this solution over Celite and removal of the solvent under vacuum afforded 80 mg of the title compound (65% yield). X-ray-quality crystals were grown by vapor diffusion of pentane onto a concentrated THF solution of this compound. This compound is highly air sensitive, and consistent with what we found with homoleptic ^{t}bpy complexes of chromium, we were unable to obtain reproducible elemental analyses for this species, even from the same crop of product. The similarity of our absorption spectrum to that reported for $[CrI_2(bpy)_2]$[6c] and our X-ray crystal structure and IR spectrum are taken as evidence for the identity and sufficient purity of the title compound.

1.4. X-ray Crystallographic Data Collection and Refinement of the Structures. Black single crystals of complexes **1** and **3** were coated with perfluoropolyether, picked up with nylon loops, and were immediately mounted in the nitrogen cold stream of the diffractometer. Graphite monochromated Mo−Kα radiation (λ = 0.71073 Å) from a Mo-target rotating-anode X-ray source was used throughout. A dark green crystal of complex **1′** was covered with Paratone oil for data collection at −173 °C on a Bruker D8 Apex diffractometer equipped with a sealed tube Mo-target X-ray source. Final cell constants were obtained from least-squares fits of several thousand strong reflections. Intensity data were corrected for absorption using intensities of redundant reflections with the program SADABS.[16] The structures were readily solved by Patterson methods and subsequent difference Fourier techniques. The Bruker ShelXTL[17] software package was used for solution of the structures, and ShelXL97[18] was used for the refinement. All non-hydrogen atoms were anisotropically refined, and hydrogen atoms were placed at calculated positions and refined as riding atoms with isotropic displacement parameters. Crystallographic data of the compounds are listed in Table 1.

A split atom model was refined to account for disorder of acetonitrile molecules in compound **1**. A total of 12 restraints were used to restrain C−N distances and N−C−C angles using DFIX and DANG instructions of ShelXL97, while thermal displacement parameters of disordered atoms were restrained with EADP. At least three severely disordered THF molecules were located in the asymmetric unit of **3**. Even a split atom model refining the THF molecules on three positions was not satisfactory. The solvent contribution was therefore removed using Platon/Squeeze.[19]

1.5. X-ray Absorption Spectroscopy. Chromium K-edge spectra were recorded at beamline 7-3 at the Stanford Synchrotron Radiation Lightsource (SSRL) or at the Australian National Beamline Facility (ANBF, beamline 20B at the Photon Factory, Tsukuba, Japan). The beam energy was 3.0 GeV (SSRL) or 2.5 GeV (ANBF), and the maximal beam current was 300 mA (SSRL) or 400 mA (ANBF). Beamline 7-3 has a double-crystal Si[220] monochromator, and an upstream Rh-coated collimating mirror that also provided harmonic rejection in combination with 30% detuning. Harmonic rejection was

dx.doi.org/10.1021/ic300882r | Inorg. Chem. 2012, 51, 6969−6982

achieved at ANBF by detuning the channel-cut Si[111] monochromator by 50%. Complexes diluted with boron nitride were pressed into 0.5 mm pellets that were supported within an Al spacer between two 38 μm Kapton tape windows (window size, 2 × 10 mm), and maintained at 10 K during data collection in a continuous flow liquid helium cryostat. Spectra were recorded in transmission mode, and represent 3−8 scan averages. Data analysis, including calibration, averaging, background subtraction, splining, and normalization of all spectra were performed using the EXAFSPAK software package.[20]

1.6. Calculations. All density functional theory (DFT) calculations were performed with the ORCA program.[21] The complexes were geometry optimized using the B3LYP functional.[22] The all-electron basis sets were those reported by the Ahlrichs group.[23] Triple-ζ-quality basis sets with one set of polarization functions (def2-TZVP) were used for the Cr metal and the nitrogen atoms coordinated to it. The remaining atoms were described by slightly smaller polarized split-valence def2-SVP basis sets that are double-ζ-quality in the valence region and contain a polarizing set of d functions on the non-hydrogen atoms.[23a,b] Auxiliary basis sets used to expand the electron density in the calculations were chosen to match the orbital basis. Electronic energies and properties were calculated at the optimized geometries using the B3LYP functional.[22] In this case the same basis sets were used. The self-consistent-field calculations were tightly converged (1×10^{-8} E_h in energy, 1×10^{-7} E_h in the density charge, and 1×10^{-7} in the maximum element of the DIIS[24] error vector). The geometry search for all complexes was carried out in redundant internal coordinates without imposing geometry constraints. Geometry optimization was considered converged after the energy change was less than 1×10^{-6} E_h, the gradient norm and maximum gradient element were smaller than 3×10^{-5} E_h Bohr^{-1}, and 1×10^{-4} E_h Bohr^{-1}, respectively, and the root-mean-square and maximum displacements of all atoms were smaller than 6×10^{-4} Bohr and 1×10^{-3} Bohr, respectively. For charged species, geometry optimizations were carried out normally as well as by applying the conductor-like screening model (COSMO)[25] to model solvation in water (dielectric constant (ε) = 80.4, refractive index = 1.33). Corresponding[26] and quasi-restricted orbitals[27] and density plots were obtained using Molekel.[28]

We used the broken symmetry (BS) approach to describe our computation results.[29] We adopt the following notation: the given system was divided into two fragments. The notation BS(m,n) refers then to a broken symmetry state with m unpaired α-spin electrons essentially on fragment 1 and n unpaired β-spin electrons localized on fragment 2. In each case, fragments 1 and 2 correspond to the metal and the ligands, respectively. In this notation the standard high-spin, open-shell solution is written as BS(m + n,0). The BS(m,n) notation refers to the initial guess to the wave function. The variational process does, however, have the freedom to converge to a solution of the form BS(m − n,0) in which effectively the n β-spin electrons pair up with n < m α-spin electrons on the partner fragment. Such a solution is then a standard $M_s \approx (m - n)/2$ spin-unrestricted Kohn−Sham solution. As explained elsewhere,[26] the nature of the solution is investigated from the corresponding orbital transformation (COT), which, from the corresponding orbital overlaps, displays whether the system should be described as a spin-coupled or a closed-shell solution.

Time-dependent DFT (TD-DFT) calculations of the Cr metal K-pre-edges were conducted as previously described.[30] For all complexes, the B3LYP functional was used in conjunction with the fully uncontracted CP(PPP) basis set for the metal,[31] def2-TZVP for the nitrogen atoms, and def2-SVP for the remaining atoms for a single-point, spin unrestricted ground state DFT calculation using the optimized coordinates. TD-DFT calculations[32] were then performed allowing only for transitions from the metal 1s orbital.[30b,32] The absolute calculated transition energies are consistently underestimated because of the shortcomings in the ability of DFT to model potentials near the nucleus. This results in the deep 1s core orbitals being too high in energy relative to the valence, thus requiring a constant shift for a given absorber. It was established that a shift of 126.10 eV for Cr K-edge is required for this regime of functional and basis sets and was applied to the transition energies. Plots were obtained using "orca_mapspc" with a line broadening of 1.0 eV for Cr K-edges. Despite the inherent restrictions in describing open-shell systems with a single determinantal reference wave function, we have found that this method is quite effective at predicting the energy and relative intensities originating from the Cr 1s orbital for these complexes.

RESULTS AND DISCUSSION

2.1. Synthesis and Characterization of New Compounds. Compound **1** has been prepared analogously to $[Cr(^t bpy)_3][PF_6]_2$ and $[Cr(tpy)_2][PF_6]_2$.[4] Combining anhydrous $CrCl_2$ and phen in degassed water generates the water-soluble species $[Cr(phen)_3]Cl_2$, and addition of aqueous degassed NH_4PF_6 results in precipitation of **1**, which is collected by filtration. The dication in **1** has been shown to possess an S = 1 ground spin state (see Supporting Information, Figure S1),[33] and it has been described as a low-spin Cr(II) species,[33,34] an assignment that has made its way into a variety of textbooks.[5] The electronic absorption spectrum of **1** is shown in Figure 1. Consistent with our

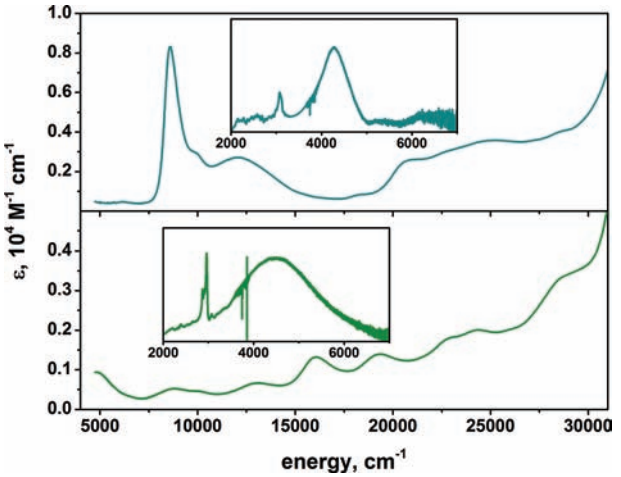

Figure 1. Electronic absorption spectra of **1** in acetonitrile (top) and **3** in THF (bottom). Insets show IR spectra taken of KBr pellets (absorption in arbitrary units).

analysis of the closely related complexes $[Cr(^t bpy)_3]^{2+}$ and $[Cr(tpy)_2]^{2+}$, which show similar absorption profiles from 10,000−25,000 cm^{-1} as the corresponding alkali-metal salt of the π-radical monoanionic ligands,[4] we assign the transitions from 7,000−25,000 cm^{-1} as intraligand transitions, requiring a description of this species as containing a central high-spin Cr(III) (d^3) ion antiferromagnetically coupled to a $[phen]_3$-centered radical monoanion. The absorption bands in this region of the spectrum are very similar to those of $[Cr^{III}(^t bpy^{\bullet})(^t bpy^0)_2]^{2+}$ and are too intense ($\varepsilon \sim 10^3$−10^4 M^{-1} cm^{-1}) to be classified as d-d transitions, although they could be interpreted as MLCT transitions if low-spin Cr(II) is invoked. However, as we will show below, this complex is indeed best described as containing a central Cr(III) ion.

Given our electronic structure assignment of **1**, ligand mixed valency should give rise to one or two low-energy intervalence charge transfer bands.[35] We have explored the absorption spectrum at lower energy (<5,000 cm^{-1}) by infrared spectroscopy (KBr pellet). As shown in the top inset of Figure 1, we do in fact observe a narrow transition centered around 4,300 cm^{-1}, the broadness of which is consistent with its assignment as an electronic transition (fwhm ~700 cm^{-1}). Unfortunately, we cannot assess the molar absorptivity of this transition using this

dx.doi.org/10.1021/ic300882r | Inorg. Chem. 2012, 51, 6969−6982

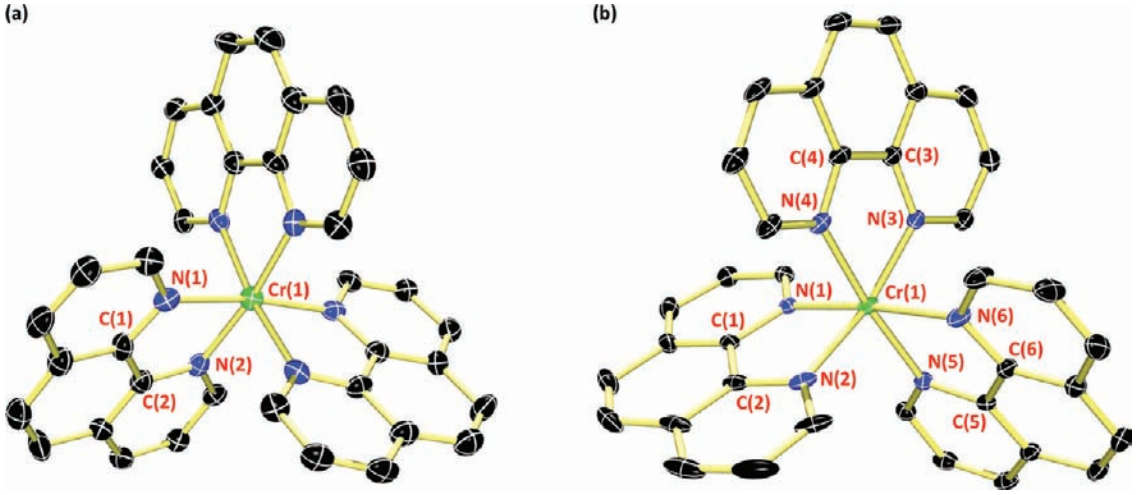

Figure 2. (a) Structure of one of the two independent dications in crystals of **1** as viewed down the crystallographic C_3 axis, which averages each of the three phen ligands. (b) Structure of the dication in **1′**, in which each of the three phen ligands are crystallographically unique.

Table 2. Crystallographically Determined Bond Lengths (Å) of the CrN_2C_2 Metallocycles[a]

	1[b]	**1′**[c]	$[Cr(phen)_3]^{3+c}$	**3**[b,c]	**4**[d]
C−C	[1.421(8)]	1.432(3);	1.430(5);	[1.470(5); 1.425(5)] [1.474(5); 1.431(5)]	1.470(5)
	[1.432(8)]	1.422(2);	1.409(8);	[1.467(5); 1.427(5)] [1.479(5); 1.433(5)]	
		1.415(2)	1.421(7)		
C−N	[1.362(6), 1.361(6)]	1.369(3), 1.373(3);	1.364(5), 1.390(5);	[1.347(4), 1.355(4); 1.384(4), 1.373(4)]	1.352(3), 1.351(4)
	[1.365(6), 1.359(6)]	1.375(3), 1.375(3);	1.390(6), 1.365(6);	[1.363(4), 1.361(4); 1.378(4), 1.376(4)]	
		1.369(3), 1.380(2)	1.367(7), 1.358(6)	[1.348(5), 1.363(4); 1.380(4), 1.367(5)]	
				[1.361(5), 1.355(5); 1.388(5), 1.368(5)]	
Cr−N	[2.049(4), 2.046(4)]	2.064(2), 2.087(2);	2.050(4), 2.040(4);	[2.069(3), 2.084(3); 2.007(3), 2.002(3)]	2.061(2), 2.062(2)
	[2.047(4), 2.045(4)]	2.065(2), 2.048(2);	2.039(4), 2.055(4);	[2.047(3), 2.060(3); 2.002(3), 2.003(3)]	
		2.024(2), 2.003(2)	2.049(4), 2.040(4)	[2.059(3), 2.077(3); 2.023(3), 2.015(3)]	
				[2.065(3), 2.054(3); 2.005(4), 2.007(4)]	

[a]Values for $[Cr^{III}(phen^0)_3]^{3+}$ and **4** are from references 36 and 15, respectively. [b]Bracketed numbers correspond to a single molecule in the unit cell. [c]A semicolon separates each metallocycle within a single molecule in the unit cell. [d]Bpy ligands are crystallographically indistinguishable.

technique. $[Cr^{III}(tpy^{\bullet})(tpy^0)]^{2+}$ (*localized* tpy-centered radical) produces a similar transition (absorption maximum at ~2,500 cm^{-1});[4b] however, the low-energy band is much narrower in **1** than in $[Cr^{III}(tpy^{\bullet})(tpy^0)]^{2+}$ (fwhm ~700 and ~2,200 cm^{-1}, respectively). Although not conclusive, we postulate that the relatively narrow bandwidth of this transition in **1** results from a more *delocalized* ligand-centered radical (Class II, II/II, or III ligand mixed valency) than was observed in $[Cr^{III}(tpy^{\bullet})(tpy^0)]^{2+}$.

We have obtained the first X-ray crystal structure of **1** (Figure 2). Unlike the crystal structures of $[Cr(^tbpy)_3]^{2+}$ and $[Cr(tpy)_2]^{2+}$ that we recently reported,[4] the crystal structure of **1** is not of sufficient quality to discern between a (localized or delocalized) ligand-centered radical or a low-spin Cr(II) species. In fact, the CrN_2C_2 metallocycle bond lengths in **1** are crystallographically indistinguishable from the same values reported for $[Cr^{III}(phen^0)_3][ClO_4]_3{\cdot}H_2O$ (Table 2).[36] Although there are two molecules of **1** in the unit cell, the three phen ligands are averaged as a consequence of the $R\bar{3}$ space group, wherein a crystallographic C_3-axis passes through the chromium centers. The same averaging was observed in the crystal structures of $[Cr(bpy)_3]^{2+}$ and $[Cr(bpy)_3]^{+}$,[37] precluding differentiation between a (localized or delocalized) ligand-centered radical or a low-spin Cr(II) species based on the structures alone. We recently reported that the corresponding crystal structures with *tert*-butyl groups in the 4 and 4′ positions of the bipyridine ligands did not suffer from this averaging, and we were able to identify one and two *localized* $(bpy^{\bullet})^-$ π-radical anionic ligands in $[Cr^{III}(^tbpy^{\bullet})(^tbpy^0)_2]^{2+}$ and $[Cr^{III}(^tbpy^{\bullet})_2(^tbpy^0)]^{+}$, respectively.

To further probe the extent of localization of the $[phen_3]$-centered radical in **1**, we sought a derivative that crystallizes in a space group that differentiates each of the three phen ligands. We have prepared the related dicationic salt of **1** with triflate counterions (**1′**) in place of hexafluorophosphate counterions. Fortunately, **1′** crystallized in the $P\bar{1}$ space group, in which all three phen ligands are crystallographically unique. The bond lengths given in Table 2 reveal that one CrN_2C_2 metallocycle is modestly distorted compared to the other two, suggesting at least partial localization of the $[phen_3]$-centered radical in **1′**. In the case of $[Cr(^tbpy)_3]^{2+}$, the metallocycle C−C and Cr−N bond lengths are most diagnostic for assigning the ligand oxidation level.[4a,9e] In **1′**, only the differences in Cr−N bond lengths of the three metallocycles are outside of the 3σ limit. Interestingly, the difference of the sum of the two Cr−N bond lengths in each metallocycle of **1′** (4.152, 4.113, and 4.027 Å) are much smaller than the differences in the same values in $[Cr(^tbpy)_3]^{2+}$ (4.130, 4.126, and 3.983 Å). This can be interpreted as arising either (1) from a greater extent of delocalization of a phen-centered radical compared to a ^{t}bpy-centered radical because of the larger π-system of phen or (2) from a more delocalized $[phen_3]$-centered radical in **1′** (Class

dx.doi.org/10.1021/ic300882r | Inorg. Chem. 2012, 51, 6969−6982

II, II/III, or III ligand mixed valency) than the [^{t}bpy$_3$]-centered radical in [Cr(^{t}bpy)$_3$]$^{2+}$ (Class I ligand mixed valency). In light of the narrowness of the absorption band of **1** at 4,300 cm^{-1}, we feel that the latter description may be operative, although both descriptions may contribute to the small bond-length differences of the three phen ligands in **1**′. It is also worth pointing out that the intraligand and CrN_2C_2 metallocycle bond lengths of the (tpy$^{\bullet}$)$^-$ and (tpy^0) ligands in [Cr^{III}(tpy$^{\bullet}$)(tpy^0)]$^{2+}$ are pronounced enough to differentiate them in the crystal structure of this complex despite the large size of the tpy π-system.[4b]

[Cr(Ar)$_2$(bpy)$_2$] (Ar is 2-methoxyphenyl) was reported by Zeiss in 1973,[6p] and [CrI$_2$(bpy)$_2$] and [Cr(NCS)$_2$(bpy)$_2$] were reported by Earnshaw and Larkworthy in 1977.[6c] X-ray crystal structures of these species have not been reported. The effective magnetic moments of these complexes are 2.58, 3.35 (3.32), and 2.91 (2.86) μ_B at 295 K (90 K), respectively, which led the authors to describe these species as low-spin Cr(II) compounds. The electronic absorption spectra of the latter compounds were reported by Earnshaw and Larkworthy but not discussed in detail, although the authors note that the absorption spectra are very similar to that of [Cr(bpy)$_3$]$^{2+}$, which we have shown possesses a central Cr(III) ion.[4a] Given our success in obtaining high-quality X-ray crystal structures with ^{t}bpy, we sought to synthesize [CrCl$_2$(^{t}bpy)$_2$] (**3**). We were pleased to find that **3** is easily prepared by the addition of 2 equiv of ^{t}bpy to anhydrous $CrCl_2$ in THF. We note that this reaction failed with bpy, 4,4′-dimethyl-2,2′-bipyridine, and phen. As shown in Supporting Information, Figure S1, compound **3** is a ground-state triplet, analogous to [Cr(Ar)$_2$(bpy)$_2$], [CrI$_2$(bpy)$_2$], and [Cr(NCS)$_2$(bpy)$_2$].

We were able to access X-ray-quality crystals of compound **3** by vapor diffusion of diethyl ether onto a THF solution of **3**. There are four independent molecules of **3** in the unit cell, each of which reveals the presence of one neutral (^{t}bpy^0) and one radical monoanionic (^{t}bpy$^{\bullet}$)$^-$ ligand (Table 2 and Figure 3); importantly, the structural differences between the neutral and monoanionic forms of the ligand were outside the 3σ limit in each case. As we have described previously, the difference between the bpy oxidation levels is easily discerned from the $C_{py}-C_{py}$ bond lengths if the crystals are of sufficient quality: ~1.49 Å for (bpy^0), ~1.43 Å for (bpy$^{\bullet}$)$^-$, and ~1.38 Å for (bpy^{2-})$^{2-}$.[9e] In crystals of **3**, the $C_{py}-C_{py}$ bonds average to 1.43 Å for the (^{t}bpy$^{\bullet}$)$^-$ ligand and 1.47 Å for the (^{t}bpy^0) ligand. Also, the $C_{py}-C_{py}$ bond length in the related species [Cr^{III}Cl$_2$(bpy^0)$_2$][PF$_6$]$_{0.62}$Cl$_{0.38}$ (**4**)[15] (1.470(5) Å, Table 2) matches with the neutral ^{t}bpy ligand in **3**. The (^{t}bpy$^{\bullet}$)$^-$ ligand in crystals of **3** is ruffled from planarity, reflecting a degree of dearomatization associated with occupation of the ^{t}bpy π^* orbital. These X-ray data are strong evidence for an electronic-structure description of **3** as [Cr^{III}Cl$_2$(^{t}bpy$^{\bullet}$)(^{t}bpy^0)], Class I (localized) ligand mixed valency. These data point to a similar electronic-structure description of the compounds reported by Zeiss,[6p] Earnshaw, and Larkworthy,[6c] namely, [Cr^{III}(Ar)$_2$(bpy$^{\bullet}$)(bpy^0)], [Cr^{III}I$_2$(bpy$^{\bullet}$)(bpy^0)], and [Cr^{III}(NCS)$_2$(bpy$^{\bullet}$)(bpy^0)].

The electronic absorption spectrum of **3** is very similar to that of [CrI$_2$(bpy)$_2$][6c] and is shown in Figure 1. The spectrum is also very similar to that of [Cr(^{t}bpy)$_3$][PF$_6$]$_2$, consistent with the report that [CrI$_2$(bpy)$_2$] and [Cr(bpy)$_3$]$^{2+}$ have nearly identical electronic absorption spectra.[6c] An important difference between the spectra of **3** and [Cr(^{t}bpy)$_3$]$^{2+}$ is the presence of an absorption band centered at ~4,800 cm^{-1} in THF (4,500 cm^{-1} in KBr, Figure 1) in compound **3** with $\varepsilon \sim 10^3$ M^{-1} cm^{-1} in THF solution. The molar absorptivity of this transition is inconsistent with an assignment as a d−d transition,[38] and we therefore assign it as an intervalence charge-transfer (IVCT) transition arising from Class I (localized) ligand mixed valency. This band is much broader than the corresponding band observed in the IR spectrum of **1** (fwhm ~1,800 cm^{-1} for **3** vs ~700 cm^{-1} for **1** in KBr), consistent with a *localized* ligand-centered radical in **3**, a conclusion that is nicely corroborated by the X-ray crystal structure.

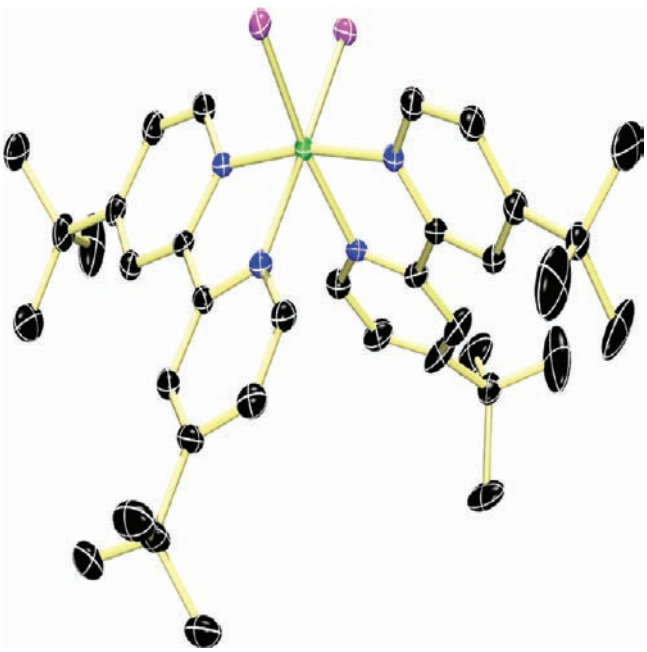

Figure 3. Structure of one of the four independent molecules in crystals of **3**.

2.2. Chromium K-Edge X-ray Absorption Spectroscopy of Compounds 1−8. The crystallographic and spectroscopic results for complexes **1** and **3** described above suggest that such compounds may have been incorrectly described in the literature.[6c,33,34] We have recently reported that the corresponding compounds [Cr(^{t}bpy)$_3$]$^{2+}$ and [Cr(tpy)$_2$]$^{2+}$ have also been incorrectly assigned as low spin Cr(II) compounds; they are, in fact, Cr(III) compounds that are antiferromagnetically coupled to a ligand-centered radical.[4] In multiple inorganic chemistry textbooks, [Cr(CN)$_6$]$^{4-}$, [Cr(bpy)$_3$]$^{2+}$, [Cr(phen)$_3$]$^{2+}$, [Cr(tpy)$_2$]$^{2+}$, and [CrX$_2$(bpy)$_2$] are listed as the only members of a small class of low-spin Cr(II) compounds,[5] although other formally low-spin Cr(II) compounds have been reported as well.[6] To the best of our knowledge, there are only four additional classes of compounds that have been described as containing a central low-spin Cr(II) ion, representative examples of which include [Cr(TPP)(py)$_2$] (**5**),[6b,11] [Cr(^{t}BuNC)$_6$]$^{2+}$ (**6**),[6d] [CrCl$_2$(dmpe)$_2$] (**7**),[12] and [Cr(Cp)$_2$] (**8**).[6a,j] Members of the last three categories seem to be legitimate examples of low-spin Cr(II) because none of the ligands in these complexes possess low-lying LUMOs that might be easily reduced. Consistent with this notion, we have already demonstrated that [Cr^{II}(CN)$_6$]$^{4-}$ is a legitimate low-spin Cr(II) complex. On the other hand, **5** may be an exception, as the radical trianion of porphyrin ligands is known.[39]

dx.doi.org/10.1021/ic300882r | *Inorg. Chem.* 2012, 51, 6969−6982

A useful tool for comparing the oxidation state (through Z_{eff}) of a given transition-metal ion across a series of compounds is X-ray absorption spectroscopy (XAS). As we have described previously, Cr K-edge XAS has provided definitive evidence that all members of the electron transfer series $[Cr(^tbpy)_3]^{3+/2+/1+/0}$ and $[Cr(tpy)_2]^{3+/2+/1+/0}$ contain a high-spin Cr(III) (d^3) center, where added electrons occupy ligand-centered orbitals in each case.[4] These results were compared against standards for high-spin Cr(II) ($[Cr(tacn)_2]Br_2$) and low-spin Cr(II) ($K_4[Cr(CN)_6]$), and a clear difference in the position of the first transition in the pre-edge region of the chromium K-edge X-ray absorption spectra was observed for compounds containing a central Cr(II) or Cr(III) ion (see Table 3). Importantly, the position of the first pre-edge transition for octahedral Cr(III) complexes is largely invariant with respect to the ligand environment (C_6, N_6, O_6, O_4Cl_2, and S_6) and overall charge (from 3− to 3+), falling between 5989.9 and 5990.7 eV in each case. While differences in position of the rising edge were discernible in some cases, the edge positions are not well-defined in these species because of the large number of transitions to 4p states and higher-energy Rydberg states that occur in the rising-edge region, and we have accordingly relied on the position of the first pre-edge transition in assigning spectroscopic oxidation states.

We felt that a full XAS study of representative members of each class of low-spin Cr(II) compounds was in order to ascertain which members had been correctly identified as low-spin Cr(II) and which had not. Here, we have measured the chromium K-edge X-ray absorption spectra of $[Cr(phen)_3][PF_6]_2$ (**1**), $[CrCl_2(^tbpy)_2]$ (**3**), $[Cr(TPP)(py)_2]$ (**5**), $[Cr(^tBuNC)_6][PF_6]_2$ (**6**), $[CrCl_2(dmpe)_2]$ (**7**), and $[Cr(Cp)_2]$ (**8**), as well as the Cr(III) reference compounds $[Cr(phen)_3][PF_6]_3$ (**2**) and $[CrCl_2(bpy)_2][PF_6]_{0.62}Cl_{0.38}$ (**4**). These data are reported in Figure 4 and Table 3.

Table 3. Comparison of Calculated and Experimentally Determined Cr K-Pre-Edge Energies (eV) of Octahedral Chromium Complexes

compound	exp	calc[a]	ref
trans-$[Cr^{III}Cl_2(OH_2)_4]Cl$	5990.6		40
$[Cr^{III}(tacn)_2]^{3+b}$	5990.4		4a
$[Cr^{III}(CN)_6]^{3-}$	5990.2		4a
$[Cr^{III}(^{3,6}L_{sq}^{\bullet})_3]^{0c}$	5990.7		40
$[Cr^{III}(^{3,6}L_{sq}^{\bullet})_2(^{3,6}L_{cat})]^{-d}$	5990.7		40
$[Cr^{III}(mnt)_3]^{3-e}$	5990.3		41
$[Cr^{III}(^tbpy^0)_3]^{3+}$	5990.4		4a
$[Cr^{III}(^tbpy^{\bullet})(^tbpy^0)_2]^{2+}$	~5990.4		4a
$[Cr^{III}(^tbpy^{\bullet})_2(^tbpy^0)]^{+}$	5990.4		4a
$[Cr^{III}(^tbpy^{\bullet})_3]^{0}$	5990.4		4a
$[Cr^{III}(tpy^0)_2]^{3+}$	5990.3		4b
$[Cr^{III}(tpy^{\bullet})(tpy^0)]^{2+}$	5989.9		4b
$[Cr^{III}(tpy^{\bullet})_2]^{+}$	5990.4		4b
$[Cr^{III}(tpy^{\bullet\bullet})(tpy^{\bullet})]^{0}$	5990.7		4b
$[Cr^{III}(phen^{\bullet})(phen^0)_2]^{2+}$ (**1**)	~5990.4	5990.6	this work
$[Cr^{III}(phen^0)_3]^{3+}$ (**2**)	5990.4	5990.4	this work
$[Cr^{III}Cl_2(^tbpy^{\bullet})(^tbpy^0)]^{0}$ (**3**)	~5990.4	5990.6	this work
$[Cr^{III}Cl_2(bpy^0)_2]^{+}$ (**4**)	5990.4	5990.5	this work
$[Cr^{III}(TPP^{3\bullet-})(py)_2]^{0}$ (**5**)	5990.6	5990.4	this work
$[Cr^{II}(^tBuNC)_6]^{2+}$ (**6**)	~5989.0	5989.3	this work
$[Cr^{II}Cl_2(dmpe)_2]^{0}$ (**7**)	~5989.5	5989.9	this work
$[Cr^{II}(Cp)_2]^{0}$ (**8**)	~5989.5[f]	~5989.2	this work
$[Cr^{II}(CN)_6]^{4-}$	5989.1		4a

[a]All calculated transitions have been increased by 126.1 eV. [b]tacn is 1,4,7-triazacyclononane. [c]$(^{3,6}L_{sq}^{\bullet})^-$ represents 3,6-di-*tert*-butylbenzosemiquinonate (1−). [d]$^{3,6}L_{cat}$ is the closed-shell one-electron-reduced form (2−) of $(^{3,6}L_{sq}^{\bullet})^-$. [e]emnt is maleonitrile dithiolate (2−). [f]The position of the first pre-edge transition is difficult to discern in this case because of the more intense transition at slightly higher energy (see section 2.4 for further discussion).

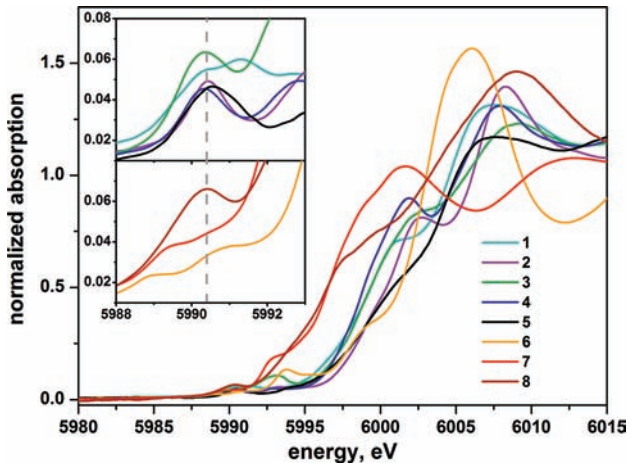

Figure 4. Normalized chromium K-edge X-ray absorption spectra of complexes **1**−**8**. The insets show expansions of the lowest-energy transitions in the pre-edge region. The top inset contains compounds that we have assigned as containing a central Cr(III) ion and the bottom inset contains compounds that we assign as true low-spin Cr(II) compounds. The dashed gray line in the insets at 5990.4 eV is meant to guide the eye to the position where octahedral Cr(III) compounds generally show their first pre-edge feature.

The position of the first pre-edge feature of octahedral Cr(III) complexes occurs at 5989.9−5990.7 eV, depending on the ligand environment (Table 3). As shown in Table 3 and Figure 4, the position of the first pre-edge feature of genuine low-spin Cr(II) complexes ($K_4[Cr^{II}(CN)_6]$ and **6**−**8**) occurs at 5989.0−5989.5 eV, depending on the ligand environment. This is consistent with the observation that a one-electron reduction of the metal center is generally accompanied by an approximately 1 eV shift to lower energy of the first pre-edge feature.[41] Complexes **1**−**5** show lowest-energy pre-edge features at 5990.4−5990.6 eV, revealing that all of these complexes contain a central Cr(III) ion. Therefore, $[CrCl_2(^tbpy)_2]$ and $[Cr(phen)_3]^{2+}$ *cannot* be described as low-spin Cr(II) species, but instead are best described as $[Cr^{III}Cl_2(^tbpy^{\bullet})(^tbpy^0)]$ (Class I (localized) ligand mixed valency) and $[Cr^{III}(phen^{\bullet})(phen^0)_2]^{2+}$ (Class II, II/III, or III ligand mixed valency), respectively. Interestingly, the first Cr K-pre-edge feature of **5** lies directly in the region expected for Cr(III) compounds (5990.6 eV), suggesting that this species was incorrectly assigned as containing a central low-spin Cr(II) ion: these XAS data reveal that the TPP^{2-} ligand, the pyridine ligands, or some combination of the TPP^{2-} and pyridine ligands must be reduced by one electron. These results provide strong evidence that low-spin Cr(II) is a legitimate description *only for the following three classes of compounds:* (1) organometallic species (containing cyclopentadienide,[6a,g,h,j−l,o] pentadienide,[61−n] allyl,[6n] and/or aryl[6o] ligands), (2) $[Cr^{II}X_2(R_3Z)_4]$,[12] and (3) $[Cr^{II}(CNR')_6]^q$ [Z = P, As; X =

dx.doi.org/10.1021/ic300882r | Inorg. Chem. 2012, 51, 6969−6982

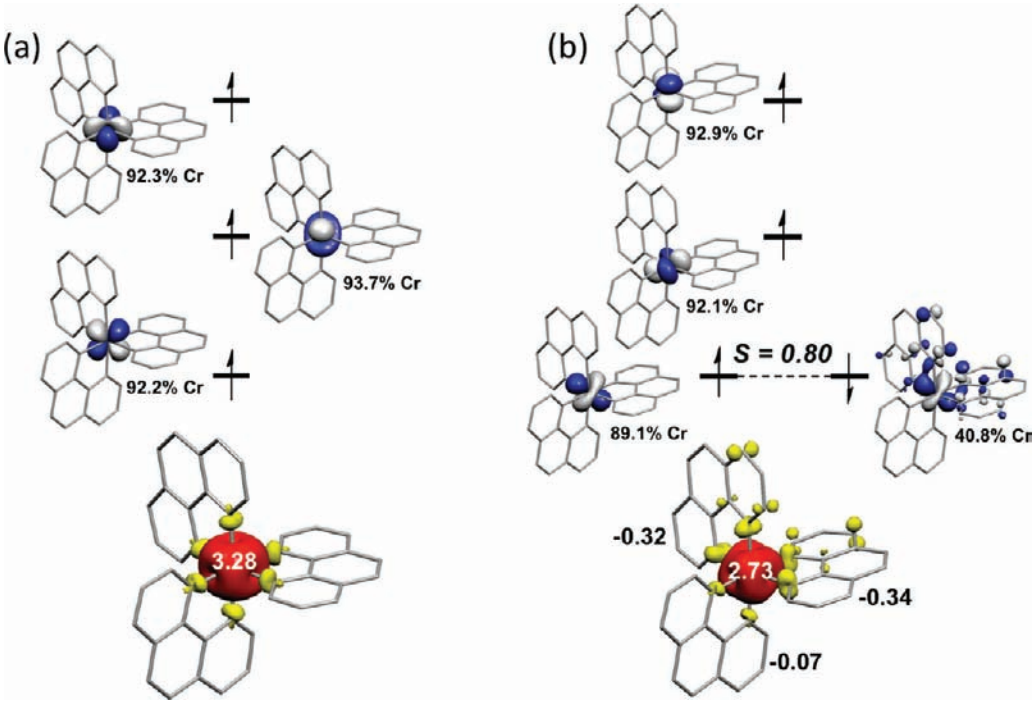

Figure 5. Qualitative MO scheme (top) and calculated Mulliken spin density (bottom) of (a) the trication in **2** and (b) the dication in **1**.

halide, CN^-, amido, or alkyl; R′ = alkyl or aryl (q = 2+)[6d] or lone pair (q = 4−)[7]].

2.3. Density Functional Theoretical Calculations. We have calculated the electronic structures of complexes **1**−**8** using (broken-symmetry) density functional theory (DFT) with the B3LYP functional. All calculations have been performed both as single-point calculations on crystal structure geometries and by geometry optimization using the crystal-structure geometry as a starting point. In each case, the qualitative electronic-structure descriptions of the single-point and geometry-optimized calculations are the same. As expected for the B3LYP functional, the chromium−ligand bond lengths are slightly overestimated following geometry optimization. As with the members of the electron transfer series $[Cr(^tbpy)_3]^l$, $[Cr(tpy)_2]^l$, $[Cr(tacn)_2]^m$, and $[Cr(CN)_6]^n$ (l = 3+, 2+, 1+, 0; m = 3+, 2+; n = 3−, 4−),[4] we have calculated the Cr K-pre-edge X-ray absorption transitions to validate our calculated electronic structure assignments by comparison to experiment. The calculated and experimental pre-edge energies are in good agreement (Table 3 and Figure 9), giving us confidence in the electronic structure assignments made from these calculations.

Figure 5 shows the calculated FMOs of compounds **1** and **2**. A Kohn−Sham spin-unrestricted (UKS) $S = {}^3/_2$ calculation of compound **2** provides the expected electronic structure of a high-spin Cr(III) (d^3) species with three half-filled singly occupied molecular orbitals (SOMOs) each of >90% Cr character. One-electron reduction of **2** provides **1**, which was investigated both by a UKS S = 1 and a broken-symmetry BS(3,1) calculation. Both calculations converged to the same solution, where the extra electron is added to an orbital of largely phenanthroline parentage, leaving the chromium center in the +III oxidation state. This ligand-centered radical is strongly antiferromagnetically coupled to the Cr(III) center yielding the observed S = 1 ground state. As with the related species $[Cr^{III}(^tbpy^{\bullet})(^tbpy^0)_2]^{2+}$,[4a] the chromium character of the *beta*-spin SOMO in the antiferromagnetically coupled pair is somewhat high and could be interpreted as arising from a small contribution of Cr(II) character. We optimized the geometry of this species starting from the crystal-structure geometry with and without the conductor-like screening model (COSMO) to mimic solvation in water,[42] as well as by perturbing the starting geometry in various ways to enforce a shortening of one of the CrN_2C_2 metallocycle C−C bond lengths in an attempt to favor convergence to a solution with a *localized* $(phen^{\bullet})^-$ ligand. Regardless of the starting geometry, each calculation converged to the same solution, with a *partially* localized phen-centered π radical anion, where the radical was mostly distributed over two of the three phen ligands. This solution may result from the preference of such calculations to converge on delocalized solutions (as we will show below for **3**),[48] although the result is consistent with our X-ray crystal structure and electronic absorption spectrum of **1** as well as the crystal structure of **1**′, all of which point to a more *delocalized* ligand-centered radical than is observed in **3**, $[Cr^{III}(^tbpy^{\bullet})(^tbpy^0)_2]^{2+}$, and $[Cr^{III}(tpy^{\bullet})(tpy^0)]^{2+}$. Although the extent of localization of the $[phen_3]$-centered radical in **1** and **1**′ remains somewhat ambiguous, the data are most consistent with either Class II, II/III, or III ligand mixed valency. At the present time, it is unclear why this species delocalizes its ligand-centered radical more than the corresponding ^{t}bpy and tpy compounds and **3**. Regardless of the extent of delocalization, our experimental and theoretical results all point toward the presence of a central Cr(III) ion in **1**, revealing that this compound has been incorrectly assigned as a low-spin Cr(II) compound.

We have also calculated the electronic structure of a truncated form of **3** where we have replaced the *tert*-butyl groups with hydrogens (namely $[CrCl_2(bpy)_2]$) using a UKS S = 1 and a broken-symmetry BS(3,1) calculation. Both calculations converged to the same solution, with a central Cr(III) ion antiferromagnetically coupled to a ligand-centered radical (Figure 6b). However, the calculations converged to a

dx.doi.org/10.1021/ic300882r | *Inorg. Chem.* 2012, 51, 6969−6982

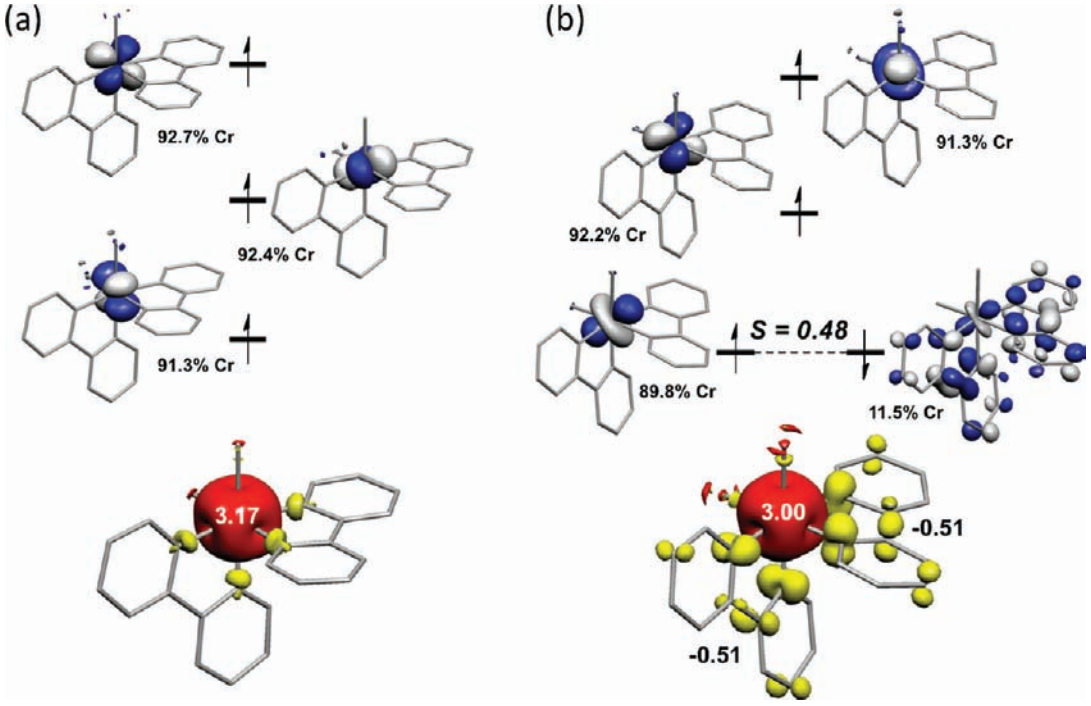

Figure 6. Qualitative MO scheme (top) and calculated Mulliken spin density (bottom) of (a) the monocation in **4** and (b) $[CrCl_2(bpy)_2]$.

solution where the $(bpy)_2$-centered radical is fully delocalized across both ligands.[48] The calculations were repeated using the conductor-like screening model (COSMO) to model solvation in water, but these also converged on a delocalized geometry.[42] On the basis of the X-ray crystal structure and electronic absorption spectrum of **3**, we have assigned this species as Class I (localized) ligand mixed valent: $[Cr^{III}Cl_2(^tbpy^{\bullet})(^tbpy^0)]$. Although we cannot reproduce the localized ligand mixed valency in our calculation, our DFT and experimental results all reveal that this complex *cannot* be described as a low-spin Cr(II) species.

For comparison with **3**, we have investigated the electronic structure of the cation in **4** by a spin-unrestricted (UKS) $S = {}^3/_2$ calculation. The relevant orbitals derived from these calculations are given in Figure 6a, which shows that this compound is a normal high-spin Cr(III) species (all three SOMOs are >90% chromium centered). Therefore, the electron added upon reduction of **4** to **3** resides in a ligand-centered orbital and couples antiferromagnetically to the central Cr(III) ion.

The electronic structure of **5** was calculated using the crystal-structure atom coordinates as an unrestricted triplet (UKS) and a broken-symmetry BS(3,1) triplet. In both the single-point and geometry-optimized solutions, the UKS and BS(3,1) calculations converged to the same solution, with a high-spin Cr(III) ($S_{Cr} = {}^3/_2$) ion antiferromagnetically coupled to a TPP-centered radical trianion ($S_{TPP} = {}^1/_2$) (Figure 7). This corroborates our experimental Cr K-edge X-ray absorption spectrum and additionally addresses the question of where the ligand-centered radical resides, namely, in a TPP-centered orbital. It is noteworthy that the TPP^{2-} ligand is preferentially reduced to the neutral pyridine ligands. We therefore demonstrate that this compound was incorrectly described as a low-spin Cr(II) species, although the experimental evidence available at the time of this assignment was not sufficient to distinguish between a low-spin Cr(II) species and a Cr(III) species antiferromagnetically coupled to a TPP-centered radical

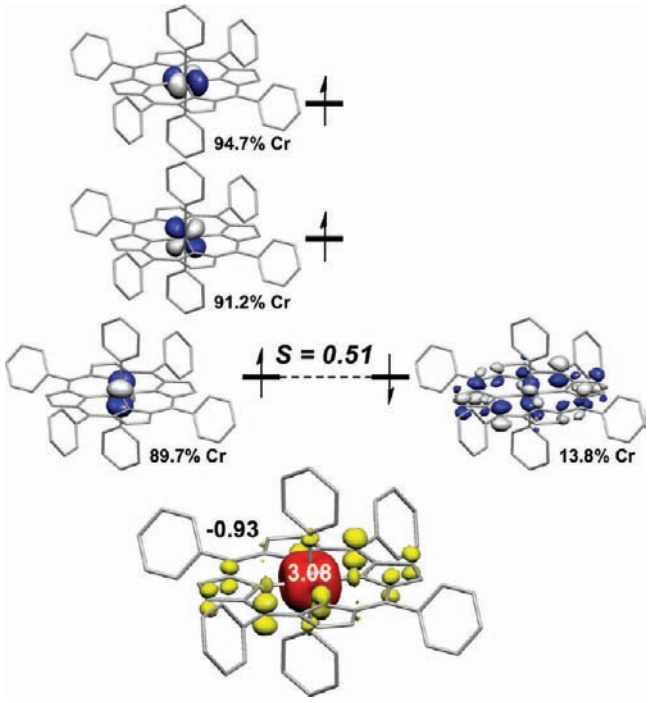

Figure 7. Qualitative MO scheme (top) and calculated Mulliken spin density (bottom) of **5**.

trianion.[39] In their original report on **5**, Reed and co-workers[6b,11] suggested that the electronic absorption spectrum of compound **5** was inconsistent with current data on complexes containing porphyrin radical trianions.[39] Reed and co-workers also isolated and fully characterized the related compound $[Cr^{II}(TPP)]$, which was shown to have a quintet ground state, as expected for square-planar Cr(II). It was suggested that coordination of two pyridine ligands to $[Cr^{II}(TPP)]$ resulted in a spin-state change from high-spin (*S*

dx.doi.org/10.1021/ic300882r | *Inorg. Chem.* 2012, 51, 6969−6982

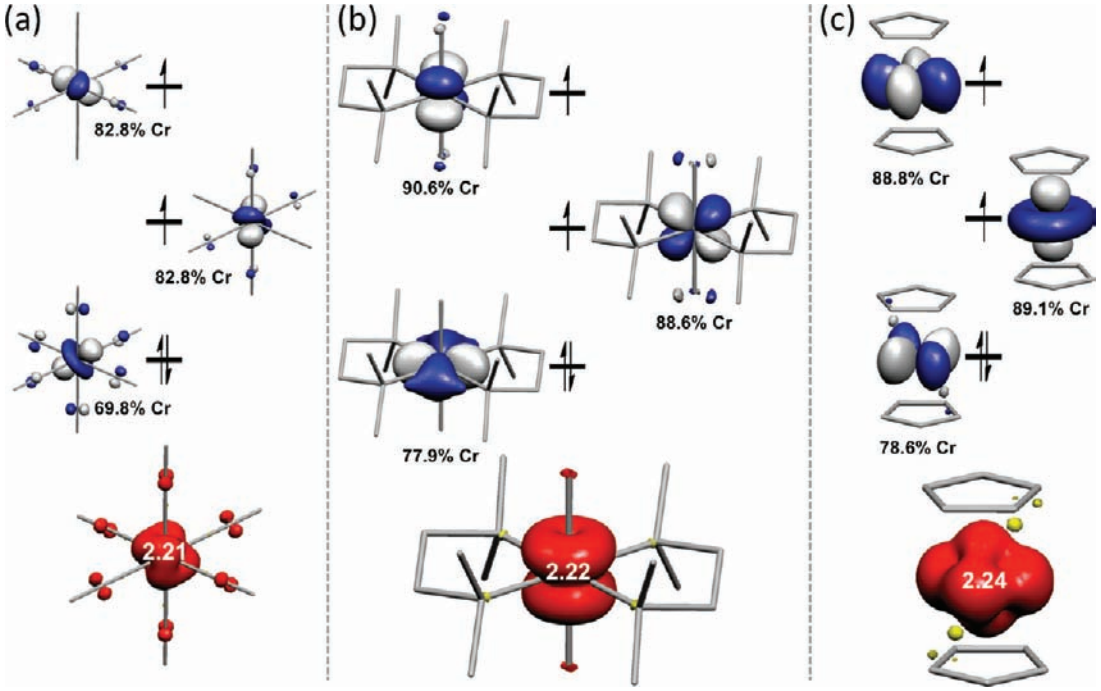

Figure 8. Qualitative MO scheme (top) and calculated Mulliken spin density (bottom) of (a) $[Cr(CNMe)_6]^{2+}$, (b) **7**, and (c) **8**.

= 2) to low-spin (S = 1) Cr(II). Our present results reveal a more dramatic change in electronic structure upon coordination of two pyridine ligands to $[Cr^{II}(TPP)]$, wherein pyridine coordination induces TPP-centered reduction by the Cr(II) ion, and the observed S = 1 spin state of **5** must, therefore, result from antiferromagnetic exchange coupling of doublet $TPP^{3\bullet-}$ with the Cr(III) center ($S_{Cr} = {}^3/_2$). Theopold recently reported a similar coordination-induced electron transfer: addition of methyl ligands (from MeLi) to a Cr(II) complex bearing an α-diimine radical monoanion induced a chromium-to-ligand electron transfer, providing a Cr(III) species coordinated to an α-diimine singlet dianion.[44a]

To qualitatively verify our electronic structure assignments of complexes **6**–**8** as true low-spin Cr(II) species, we have calculated the electronic structure of geometry-optimized $[Cr(MeNC)_6]^{2+}$ (as a model for **6** where the *tert*-butyl groups have been replaced by methyl groups), **7**, and **8**. Our electronic-structure calculations reveal that these are indeed well described as true low-spin Cr(II) species (the two SOMOs and the HOMO are of ≥70% Cr character), in agreement with our Cr K-edge X-ray absorption spectra. Relevant frontier molecular orbitals are shown in Figure 8. These calculations are consistent with the notion that isonitrile, phosphine, and cyclopentadienide ligand are strong-field ligands capable of stabilizing low-valent transition metals in low-spin electron configurations; these ligands do not have the energetically low-lying unoccupied orbitals that can accept a single electron as do bpy, phen, tpy, and TPP^{2-}.

2.4. Calculated Cr K-Pre-Edge X-ray Absorption Spectra. In an effort to assess the quality and reliability of our electronic structure calculations, we have calculated the Cr K-pre-edge X-ray absorption spectra of these complexes using time-dependent DFT (TD-DFT) for comparison with the experimental data described above. Following an empirical 126.10 eV adjustment of the calculated spectra, good agreement of the position of the first pre-edge feature is achieved, as shown in Figure 9. We have relied most heavily on

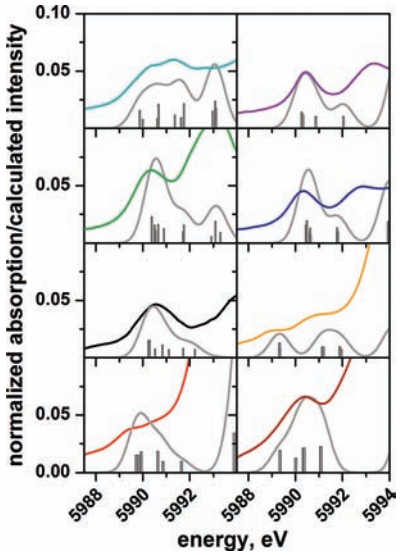

Figure 9. Comparison of calculated (gray) and experimental chromium K-pre-edge X-ray absorption spectra of complexes **1**–**8**. Columns depict the calculated transitions; calculated intensities are given in arbitrary units.

the position of the lowest-energy pre-edge feature for oxidation-state assignments of such octahedral chromium compounds because the energy of this transition, which involves $1s(\beta) \rightarrow t_{2g}(\beta)$ excitation, is very oxidation-state dependent and is largely insensitive to ligand identity and overall charge (Table 3).[4,40,41] It is established that this TD-DFT methodology does not accurately predict X-ray absorption features involving high charge-transfer character (e.g., MLCT),[43] and we accordingly are not concerned with computationally reproducing the higher-energy pre-edge features observed in our experimental spectra. The agreement between calculated and experimental Cr K-pre-edge X-ray absorption spectra shown in Figure 9 demonstrates that the

dx.doi.org/10.1021/ic300882r | Inorg. Chem. 2012, 51, 6969–6982

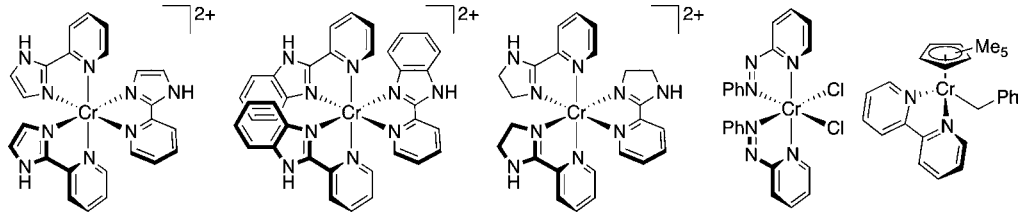

Figure 10. Other literature compounds incorrectly assigned as containing a central low-spin Cr(II) ion. The left three complexes have not been crystallized, and one isomer of each species is shown, although the actual structures are unknown. These species are from refs 6e, 6f, and 6q.

computationally derived electronic structures of complexes **1**−**8** are reliable.

It is worth pointing out that the pre-edge X-ray absorption profile of **8** is well reproduced by TD-DFT, and the calculated spectrum highlights that the first pre-edge transition occurs at lower energy than the first-peak maximum near 5990.2 eV. Therefore, while it appears from the X-ray absorption spectrum of **8** that this species might be classified as a Cr(III) complex, this is likely due to a masking of the lowest-energy transition by more-intense, slightly higher-energy transitions around 5990.2 eV. Importantly, the lowest-energy transition calculated for complexes **1**−**5**, which contain Cr(III) centers, are all at higher energy than the corresponding transitions for complexes **6**−**8**, which all contain genuine low-spin Cr(II) centers.

2.5. Low-Spin Chromium(II) Compounds. As described above, a variety of compounds have been described as low-spin Cr(II) species. However, when such species possess ligands with energetically low-lying LUMOs (e.g., bpy, tpy, phen, TPP^{2-}, and alpha-diimines[44]), a description involving Cr(III) antiferromagnetically coupled to a one-electron-reduced ligand set is more appropriate. There are, to our knowledge, five other complexes that have been incorrectly described as containing a central low-spin Cr(II) ion (Figure 10). The first three complexes are homoleptic dicationic chromium complexes bearing 2,2′-pyridineimidazole, 2,2′-pyridinebenzimidazole, and 2,2′-pyridineimidazoline ligands.[6f] None of these complexes have been characterized by crystallography; however, their reported absorption spectra match very closely with that of the dication $[Cr^{III}(bpy^{\bullet})(bpy^{0})_2]^{2+}$, suggesting that all four complexes have a similar electronic structure involving a central Cr(III) ion. The fourth compound that has been incorrectly described as containing a central low-spin Cr(II) ion is $[CrCl_2(pap)_2]$, where pap is 2-(phenylazo)pyridine.[6e,i,k] This compound and its derivatives have been characterized by X-ray crystallography. The bidentate pap ligand binds through the pyridine nitrogen and the phenyl-bearing azo nitrogen. The crystal structure of $[CrCl_2(pap)_2]$ reveals one long and one short N−N bond (1.314(2) and 1.282(2) Å).[6e] The crystal structure of a closely related compound, in which the phenyl group on one pap ligand is replaced with a 4-(phenylamino)-pheny group, also reveals one long and one short N−N bond (1.326(5) Å for the pap azo bond and 1.288(5) Å for the substituted-pap azo bond).[6k] The ability of azo-pyridine ligands to stabilize "low-spin Cr(II)" has been attributed to the high π-acidity of this ligand.[6e,45] However, the localized reduction of one of the two pap ligands in $[CrCl_2(pap)_2]$ is analogous to what we have observed in **3**, $[Cr^{III}(^{t}bpy^{\bullet})(^{t}bpy^{0})_2]^{2+}$, and $[Cr^{III}(tpy^{\bullet})(tpy^{0})]^{2+}$, which points to a similar electronic structure involving a central Cr(III) ion in each case. Also, Goswami and co-workers have clearly demonstrated that pap is a redox noninnocent ligand and that the electronic structure of the homoleptic neutral species $[Cr(pap)_3]^0$ is best described as $[Cr^{III}(pap^{\bullet})_3]^0$.[46] Therefore, $[CrCl_2(pap)_2]$ should not be described as a low-spin Cr(II) species, but instead as a Cr(III) species antiferromagnetically coupled to a *localized* (Class I ligand mixed valency) pap-centered radical monoanion. Finally, the fifth compound that has been incorrectly identified as a low-spin Cr(II) species is [Cp*Cr(Bn)(bpy)] (Bn is benzyl).[6q] The X-ray crystal structure of this species revealed that the $C_{py}-C_{py}$ bond is short, at 1.40(1) Å, directly in the region expected for a bpy-centered radical monoanion.[4a,9e] Therefore, the electronic structure of this compound is best described as $[Cp^{*}Cr^{III}(Bn)(bpy^{\bullet})]$.

Finally, after refining the scope of low-spin Cr(II), there remains a number of species that are legitimate low-spin Cr(II) species (Figure 11). A unifying feature of each species is the

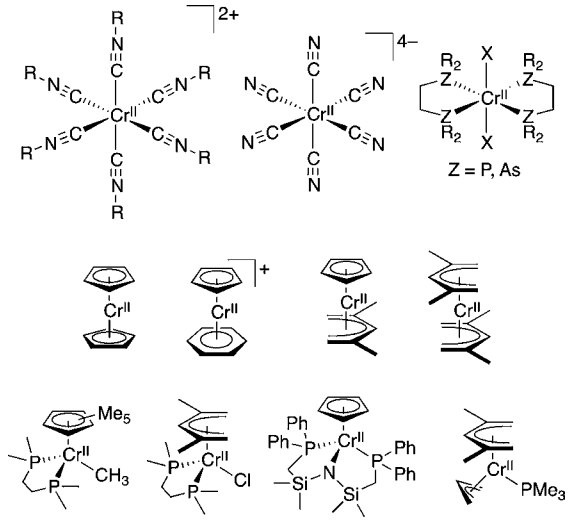

Figure 11. Legitimate low-spin Cr(II) complexes in the literature.

presence of ligands in the strong-field extreme of the spectrochemical series (phosphine,[6g,h,m,n,12b−j] arsine,[12a] cyanide,[7] isonitrile,[6d] pentadienide,[6l−n] allyl,[6n] aryl,[6o] and cyclopentadienide[6a,g,h,j−l,o]). It is noteworthy that $[CrI_2(depe)_2]$ (depe is 1,2-bis(diethylphosphino)ethane)[12e] and certain derivatives of chromocene[47] have been shown to undergo spin crossover to high-spin Cr(II) at temperatures above 100 K. In the case of $[CrX_2(R_2PCH_2CH_2PR_2)_2]$, only the diiodide species has been observed to undergo spin crossover, where the inflection point in effective magnetic moment occurs near 170 K. It is noteworthy that, even in the presence of strong-field ligands such as phosphines and cyclopentadienide derivatives, Cr(II) species can still adopt a high-spin configuration at elevated temperatures, revealing how difficult true low-spin Cr(II) species are to stabilize.

dx.doi.org/10.1021/ic300882r | *Inorg. Chem.* 2012, 51, 6969−6982

CONCLUSIONS

The studies presented in this Article reveal that low-spin Cr(II) complexes are more rare than previously believed. The present results and recent papers from our research group[4] have firmly demonstrated that, if ligands with low-lying LUMOs are coordinated to a chromium center, a central low-spin Cr(II) ion should not be invoked, as an electron most certainly resides in a ligand-centered LUMO. However, the strong-field ligands CN^-, isonitriles, phosphines, arsines, pentadienide, allyl, aryl, and cyclopentadienide derivatives are able to stabilize a low-spin (S = 1) Cr(II) center. We therefore demonstrate that, to our knowledge, only three classes of legitimate low-spin Cr(II) species have been synthesized: (1) organometallic species (containing cyclopentadienide,[6a,g,h,j−l,o] pentadienide,[6l−n] allyl,[6n] and/or aryl[6o] ligands), (2) $[Cr^{II}X_2(R_3Z)_4]$,[12] and (3) $[Cr^{II}(CNR')_6]^q$ [Z = P, As; X = halide, CN^-, amido, or alkyl; R′ = alkyl or aryl (q = 2+)[6d] or lone pair (q = 4−)[7]].

ASSOCIATED CONTENT

Supporting Information

Temperature dependence of the magnetic moments of **1** and **3**; crystallographic information files (cif) of complexes **1**, **1′**, and **2**; geometry-optimized coordinates; and calculated Cr 3d and 4p contributions to acceptor orbitals from calculated (TD-DFT) X-ray absorption spectra. This material is available free of charge via the Internet at http://pubs.acs.org.

AUTHOR INFORMATION

Corresponding Author

*E-mail: scarborough@emory.edu (C.C.S.), wieghardt@mpi-muelheim.mpg.de (K.W.).

Notes

The authors declare no competing financial interest.

ACKNOWLEDGMENTS

We thank Heike Schucht and Andreas Göbels for technical assistance, Kyle M. Lancaster for preliminary XAS experiments, and Leah H. Schlientz for preparation of **1′**. C.S. is grateful to the Alexander von Humboldt Foundation for a postdoctoral fellowship. Portions of this research were carried out at the Stanford Synchrotron Radiation Lightsource, a Directorate of SLAC National Accelerator Laboratory and an Office of Science User Facility operated by the U.S. Department of Energy Office of Science by Stanford University. The SSRL Structural Molecular Biology Program is supported by the DOE Office of Biological and Environmental Research, and by the National Institutes of Health, National Center for Research Resources, Biomedical Technology Program. Additional research was undertaken at the Australian National Beamline Facility (ANBF) at the Photon Factory in Japan, operated by the Australian Synchrotron (AS). We acknowledge the Australian Research Council for financial support and the High Energy Accelerator Research Organisation (KEK) in Tsukuba, Japan, for operations support. C.D. is grateful for travel funding provided by the International Synchrotron Access Program (ISAP) managed by the AS and funded by the Australian Government.

REFERENCES

(1) Hegedus, L. S. In *Transition Metals in the Synthesis of Complex Organic Molecules*; University Science Books: Mill Valley, CA, 1994; p 3.

(2) (a) Jörgensen, C. K. *Oxidation Numbers and Oxidation States*; Springer: Berlin, Germany, 1969. (b) Bill, E.; Bothe, E.; Chaudhuri, P.; Chlopek, K.; Herebian, D.; Kokatam, S.; Ray, K.; Weyhermüller, T.; Neese, F.; Wieghardt, K. *Chem.—Eur. J.* **2005**, *11*, 204−224.

(3) In this manuscript we use the term "low-spin Cr(II)" in reference to octahedral symmetry, in which four electrons are placed in the t_{2g} orbitals to provide an overall S = 1 spin state. Triplet octahedral Cr(II) species are more correctly described as "intermediate spin" (Alvarez, S.; Cirera, J.*Angew. Chem., Int. Ed.* **2006**, *45*, 3012−3020). However, we adopt the description of these complexes as "low spin", as they have been exclusively described this way in the literature. A number of so-called "low-low-spin Cr(II)" complexes (S = 0) have been reported, including $[Cr^{II}(CN^tBu)_7]^{2+}$ (Mialki, W. S.; Wigley, D. E.; Wood, T. E.; Walton, R. A. *Inorg. Chem.* **1982**, *21*, 480−485), $[CpCr^{II}(CNR)_4]^+$ (Shen, J. K.; Freeman, J. W.; Hallinan, N. C.; Rheingold, A. L.; Arif, A. M.; Basolo, F. *Organometallics* **1992**, *11*, 3215−3224, and Heigl, O. M.; Herdtweck, E.; Grasser, S.; Köhler, F. H.; Strauss, W.; Zeh, H. *Organometallics* **2002**, *21*, 3572−3579), $CpCr^{II}X(CO)_3$ and corresponding phospine and allyl complexes (for example: Normal, D. W.; Ferguson, M. J.; Stryker, J. M. *Organometallics* **2004**, *23*, 2015−2019. Jaeger, T. J.; Baird, M. C. *Organometallics* **1988**, *7*, 2074−2076. Malisch, W.; Alsmann, R. *Angew. Chem.* **1976**, *88*, 809−810. Hackett, P.; O'Neill, P. S.; Manning, A. R. *J. Chem. Soc., Dalton Trans.* **1974**, 1625−1627. King, R. B.; Efraty, A.; Douglas, W. M. *J. Organomet. Chem.* **1973**, *60*, 125−137. Manning, A. R.; Thornhill, D. J. *J. Chem. Soc. A: Inorg. Phys. Theor.* **1971**, 637−639), and diamagnetic Cr^{II} nitrosyl complexes; for example: Jandciu, E. W.; Kuzelka, J.; Legzdins, P.; Rettig, S. J.; Smith, K. M. *Organometallics* **1999**, *18*, 1994−2004. Bradley, D. C.; Newing, C. W. *J. Chem. Soc. D: Chem. Commun.* **1970**, 219−220.

(4) (a) Scarborough, C. C.; Sproules, S.; Weyhermüller, T.; DeBeer, S.; Wieghardt, K. *Inorg. Chem.* **2011**, *50*, 12446−12462. (b) Scarborough, C. C.; Lancaster, K. M.; DeBeer, S.; Weyhermüller, T.; Sproules, S.; Wieghardt, K. *Inorg. Chem.* **2012**, *51*, 3718−3732.

(5) (a) Larkworthy, L. F.; Nolan, K. B.; O'Brien, P. In *Comprehensive Coordination Chemistry*; Wilkinson, G., Gillard, R. D., McCleverty, J. A., Eds.; Pergamon Press: New York, 1987; Vol. 3, p 712. (b) Greenwood, N. N.; Earnshaw, A., *Chemistry of the Elements*; Wheaton, A. & Co. Ltd.: Exeter, Great Britain, 1988; p 1201. (c) Hollemann, F.; Wiberg, E. *Lehrbuch der Anorganischen Chemie*; deGruyter: Berlin, Germany, 1995; p 1455. (d) Cotton, F. A.; Wilkinson, G.; Murillo, C. A. *Advanced Inorganic Chemistry*, 6th ed.; J. Wiley & Sons: New York, 1999; p 742.

(6) (a) Weiss, E.; Fischer, E. O. *Z. Anorg. Allg. Chem.* **1956**, *284*, 69−72. (b) Cheung, S. K.; Grimes, C. J.; Wong, J.; Reed, C. A. *J. Am. Chem. Soc.* **1976**, *98*, 5028−5030. (c) Earnshaw, A.; Larkworthy, L. F.; Patel, K. C.; Tucker, B. J. *J. Chem. Soc., Dalton Trans.* **1977**, 2209−2212. (d) Mialki, W. S.; Wigley, D. E.; Wood, T. E.; Walton, R. A. *Inorg. Chem.* **1982**, *21*, 480−485. (e) Ferreira, V.; Krause, R. A.; Larsen, S. *Inorg. Chim. Acta* **1988**, *145*, 29−38. (f) de Castro, B.; Freire, C. *Synth. React. Inorg., Met.-Org. Chem.* **1990**, *20*, 1−12. (g) Thomas, B. J.; Noh, S. K.; Schulte, G. K.; Sendlinger, S. C.; Theopold, K. H. *J. Am. Chem. Soc.* **1991**, *113*, 893−902. (h) Fryzuk, M. D.; Leznoff, D. B.; Rettig, S. J. *Organometallics* **1995**, *14*, 5193−5202. (i) Kharmawphlang, W.; Choudhury, S.; Deb, A. K.; Goswami, S. *Inorg. Chem.* **1995**, *34*, 3826−3828. (j) Flower, K. R.; Hitchcock, P. B. *J. Organomet. Chem.* **1996**, *507*, 275−277. (k) Kamar, K. K.; Saha, A.; Castiñeiras, A.; Hung, C.-H.; Goswami, S. *Inorg. Chem.* **2002**, *41*, 4531−4538. (l) Köhler, F. H.; Mölle, R.; Strauss, W.; Weber, B.; Gedridge, R. W.; Basta, R.; Trakarnpruk, W.; Tomaszewski, R.; Arif, A. M.; Ernst, R. D. *Organometallics* **2003**, *22*, 1923−1930. (m) Newbound, T. D.; Freeman, J. W.; Wilson, D. R.; Kralik, M. S.; Patton, A. T.; Campana, C. F.; Ernst, R. D. *Organometallics* **1987**, *6*, 2432−2437. (n) Jolly, P. W.; Krüger, C.; Zakrewski, U. *J. Organomet. Chem.* **1991**, *412*, 371−380. (o) Köhler, F. H.; Metz, B.; Strauss, W. *Inorg. Chem.* **1995**, *34*, 4402−4413. (p) Sneedon, R. P. A.; Zeiss, H. H. *J. Organomet. Chem.* **1973**, *47*, 125−131. (q) Bhandari, G.; Kim, Y.; McFarland, J. M.; Rheingold, A. L.; Theopold, K. H. *Organometallics* **1995**, *14*, 738−745.

(7) Eaton, J. P.; Nicholls, D. *Trans. Met. Chem.* **1981**, *6*, 203−206.
(8) Cyanide is generally considered to be a redox innocent ligand and a strong π-acceptor. This distinction implies that electron density may be delocalized from a transition-metal ion into the π-system of cyanide, but generation of the radical dianionic form of cyanide by oxidation of the metal center to which it is coordinated is not feasible. There are two examples where cyanide has been reduced by a coordinated transition-metal ion resulting in cyanide C−C bond formation: (a) Shores, M. P.; Long, J. R. *J. Am. Chem. Soc.* **2002**, *124*, 3512−3513. (b) Fox, A. R.; Cummins, C. C. *Chem. Commun.* **2012**, *48*, 3061−3063. Also, the ion $[Co(CN)_3]^{6-}$ has been shown to contain a central Co^{-} ion and a $[(CN)_3]^{5-}$ unit, implying substantial cyanide reduction: (c) Höhn, P.; Jach, F.; Karabiyik, B.; Prots, Y.; Agrestini, S.; Wagner, F. R.; Ruck, M.; Tjeng, L. H.; Kniep, R. *Angew. Chem., Int. Ed.* **2011**, *50*, 9361−9364. However, this ion is predicted to be diamagnetic, consistent with the inaccessibility of metal complexes bearing *radical* dianionic cyanide ligands
(9) (a) Chisholm, M. H.; Kober, E. M.; Ironmonger, D. J.; Thornton, P. *Polyhedron* **1985**, *4*, 1869−1874. (b) Lentz, M. R.; Fanwick, P. E.; Rothwell, I. P. *Organometallics* **2003**, *22*, 2259−2266. (c) Radonovich, L. J.; Eyring, M. W.; Groshens, T. J.; Klabunde, K. J. *J. Am. Chem. Soc.* **1982**, *104*, 2816−2819. (d) Rosa, P.; Mézailles, N.; Ricard, L.; Mathey, F.; Le Floch, P. *Angew. Chem., Int. Ed.* **2000**, *39*, 1823−1826. (e) Scarborough, C. C.; Wieghardt, K. *Inorg. Chem.* **2011**, *50*, 9773−9793.
(10) (a) Hancock, R. D.; McDougall, G. J. *J. Chem. Soc., Dalton Trans.* **1977**, 67−70. (b) Josephsen, J.; Schäffer, C. E. *Acta Chem. Scand. A* **1977**, *31*, 813−824. (c) Tom Dieck, H.; Franz, K.-D.; Hohmann, F. *Chem. Ber.* **1975**, *108*, 163−173.
(11) Scheidt, W. R.; Brinegar, A. C.; Kirner, J. F.; Reed, C. A. *Inorg. Chem.* **1979**, *18*, 3610−3612.
(12) (a) Mani, F.; Stoppioni, P.; Sacconi, L. *J. Chem. Soc., Dalton Trans.* **1975**, 461−463. (b) Girolami, G. S.; Salt, J. E.; Wilkinson, G.; Thornton-Pett, M.; Hursthouse, M. B. *J. Am. Chem. Soc.* **1983**, *105*, 5954−5956. (c) Girolami, G. S.; Wilkinson, G.; Galas, A. M. R.; Thornton-Pett, M.; Hursthouse, M. B. *J. Chem. Soc., Dalton Trans.* **1985**, 1339−1348. (d) Salt, J. E.; Wilkinson, G.; Motevalli, M.; Hursthouse, M. B. *J. Chem. Soc., Dalton Trans.* **1986**, 1141−1154. (e) Halepoto, D. M.; Holt, D. G. L.; Larkworthy, L. F.; Leigh, G. J.; Povey, D. C.; Smith, G. W. *J. Chem. Soc., Chem. Commun.* **1989**, 1322−1323. (f) Arif, A. M.; Hefner, J. G.; Jones, R. A.; Koschmieder, S. U. *J. Coord. Chem.* **1991**, *23*, 13−19. (g) Ricci, G.; Forni, A.; Boglia, A.; Sonzogni, M. *Organometallics* **2004**, *23*, 3727−3732. (h) Berben, L. A.; Kozimor, S. A. *Inorg. Chem.* **2008**, *47*, 4639−4647. (i) López-Hernández, A.; Venkatesan, K.; Schmalle, H.; Berke, H. *Monatsh. Chem.* **2009**, *140*, 845−857. (j) Karunadasa, H. I.; Arquero, K. D.; Berben, L. A.; Long, J. R. *Inorg. Chem.* **2010**, *49*, 4738−4740.
(13) Robin, M. B.; Day, P.; Emeleus, H. J.; Sharpe, A. G. *Adv. Inorg. Chem.* **1968**, *10*, 247−422.
(14) Demadis, K. D.; Hartshorn, C. M.; Meyer, T. J. *Chem. Rev.* **2001**, *101*, 2655−2686.
(15) Kar, T.; Liao, M.-S.; Biswas, S.; Sarkar, S.; Dey, K.; Yap, G. P. A.; Kreisel, K. *Spectrochim. Acta, Part B* **2006**, *65*, 882−886.
(16) Sheldrick, G. M. *SADABS, Bruker-Siemens Area Detector Absorption and Other Correction*, Version 2008/1; University of Göttingen: Göttingen, Germany, 2006.
(17) *ShelXTL*, 6.14; Bruker AXS Inc.: Madison, WI, 2003.
(18) Sheldrick, G. M. *ShelXL97*; University of Göttingen: Göttingen, Germany, 1997.
(19) Spek, A. L. *Acta Crystallogr.* **2009**, *D65*, 148−155.
(20) George, G. N. *EXAFSPAK*; Stanford Synchrotron Radiation Laboratory, Stanford Linear Accelerator Center, Stanford University: Stanford, CA, 2000.
(21) Neese, F. *Orca, an Ab Initio, Density Functional, and Semiempirical Electronic Structure Program Package*, version 2.8; Universität Bonn: Bonn, Germany, 2011.
(22) (a) Becke, A. D. *Phys. Rev. A* **1988**, *38*, 3098−3100. (b) Schäfer, A.; Horn, H.; Ahlrichs, R. *J. Chem. Phys.* **1992**, *97*, 2571−2577.
(23) (a) Becke, A. D. *J. Chem. Phys.* **1993**, *98*, 5648−5652. (b) Lee, C. T.; Yang, W. T.; Parr, R. G. *Phys. Rev. B* **1988**, *37*, 785−789. (c) Schäfer, A.; Huber, C.; Ahlrichs, R. *J. Chem. Phys.* **1994**, *100*, 5829−5835.
(24) (a) Pulay, P. *Chem. Phys. Lett.* **1980**, *73*, 393−398. (b) Pulay, P. *J. Comput. Chem.* **1982**, *3*, 556−560.
(25) Klamt, A.; Jonas, V.; Burger, T.; Lohrenz, J. C. W. *J. Phys. Chem. A* **1998**, *102*, 5074−5085.
(26) Neese, F. *J. Phys. Chem. Solids* **2004**, *65*, 781−785.
(27) Schöneboom, J. C.; Neese, F.; Thiel, W. *J. Am. Chem. Soc.* **2005**, *127*, 5840−5853.
(28) *Molekel, Advanced Interactive 3D-Graphics for Molecular Sciences*; Swiss National Supercomputing Center: Manno, Switzerland; http://www.cscs.ch/molekel.
(29) (a) Noodleman, L. *J. Chem. Phys.* **1981**, *74*, 5737−5743. (b) Noodleman, L.; Case, D. A.; Aizman, A. *J. Am. Chem. Soc.* **1988**, *110*, 1001−1005. (c) Noodleman, L.; Davidson, E. R. *Chem. Phys.* **1986**, *109*, 131−143. (d) Noodleman, L.; Norman, J. G.; Osborne, J. H.; Aizman, A.; Case, D. A. *J. Am. Chem. Soc.* **1985**, *107*, 3418−3426. (e) Noodleman, L.; Peng, C. Y.; Case, D. A.; Mouesca, J. M. *Coord. Chem. Rev.* **1995**, *144*, 199−244.
(30) (a) DeBeer George, S.; Petrenko, T.; Neese, F. *Inorg. Chim. Acta* **2008**, *361*, 965−972. (b) DeBeer George, S.; Petrenko, T.; Neese, F. *J. Phys. Chem. A* **2008**, *112*, 12936−12943.
(31) Neese, F. *Inorg. Chim. Acta* **2002**, *337*, 181−192.
(32) (a) Berry, J. F.; DeBeer George, S.; Neese, F. *Phys. Chem. Chem. Phys.* **2008**, *10*, 4361−4374. (b) Yano, J.; Robblee, J.; Pushkar, Y.; Marcus, M. A.; Bendix, J.; Workman, J. M.; Collins, T. J.; Solomon, E. I.; George, S. D.; Yachandra, V. K. *J. Am. Chem. Soc.* **2007**, *129*, 12989−13000.
(33) (a) Earnshaw, A.; Larkworthy, L. F.; Patel, K. C.; Patel, K. S.; Carlin, R. L.; Terezakis, E. G. *J. Chem. Soc. A: Inorg. Phys. Theor.* **1966**, 511−513. (b) Lutz, P. B.; Long, G. J.; Baker, W. A. *Inorg. Chem.* **1969**, *8*, 2529−2531.
(34) (a) Hughes, M. C.; Macero, D. J. *Inorg. Chem.* **1976**, *15*, 2040−2044. (b) La Mar, G. N.; Van Hecke, G. R. *J. Am. Chem. Soc.* **1969**, *91*, 3442−3450. (c) La Mar, G. N.; Van Hecke, G. R. *Inorg. Chem.* **1973**, *12*, 1767−1773. (d) Percy, G. C.; Thornton, D. A. *J. Mol. Struct.* **1971**, *10*, 39−48.
(35) In idealized D_3 symmetry, the three phen-centered LUMOs transform as $a_1 + e$. If the e set is energetically lower than the a_1 orbital, a Jahn−Teller-active species would result in lowering the symmetry of this species to C_2. In such a case, these orbitals would transform as $a + a + b$ with one of these as a SOMO and the other two unoccupied, resulting in two intervalence charge-transfer transitions. On the other hand, if the orbital of a_1 symmetry is energetically lower than the orbitals of e symmetry in the D_3 point group, no Jahn−Teller distortion would be expected, and a single intervalence charge transfer band would result.
(36) Luck, R. L.; Gawryszewska, P.; Riehl, J. P. *Acta Crystallogr., Sect. C: Cryst. Struct. Commun.* **2000**, *56*, E238−E239.
(37) Breu, J.; Zwicknagel, A. *Z. Naturforsch., B: Chem. Sci.* **2004**, *59*, 1015−1025.
(38) A very low-energy d−d band would be expected if this compound were low-spin Cr(II), arising from the d orbitals of π symmetry transforming as $a + a + b$ in C_2 symmetry. One such orbital would be doubly occupied and the others would be SOMOs, and excitation of the β-spin electron in the doubly occupied orbital to the SOMOs would give rise to two very low-energy ligand-field transitions. However, the intensity of this transition ($\sim$1,000 M^{-1} cm^{-1}) is much too high to support the assignment of this band as a ligand-field transition.
(39) Fuhrhup, J.-H. *Struct. Bonding (Berlin)* **1974**, *18*, 1−67.
(40) Kapre, R. R.; Bothe, E.; Weyhermüller, T.; DeBeer George, S.; Muresan, N.; Wieghardt, K. *Inorg. Chem.* **2007**, *46*, 7827−7839.
(41) Banerjee, P.; Sproules, S.; Weyhermüller, T.; DeBeer George, S.; Wieghardt, K. *Inorg. Chem.* **2009**, *48*, 5829−5847.
(42) COSMO(water) had provided the localized tpy-centered radical in $[Cr(tpy^{\bullet})(tpy^{0})]^{2+}$ that was observed in the crystal structure of this

species, whereas omission of COSMO(water) gave a solution with a delocalized [tpy_2]-centered radical (reference 4b).
(43) (a) Neese, F. *J. Biol. Inorg. Chem.* **2006**, *11*, 702−711. (b) Roemelt, M.; Beckwith, M. A.; Duboc, C.; Collomb, M.-N.; Neese, F.; DeBeer, S. *Inorg. Chem.* **2011**, *51*, 680−687. (c) Tozer, D. J. *J. Chem. Phys.* **2003**, *119*, 12697−12699.
(44) (a) Kreisel, K. A.; Yap, G. P. A.; Theopold, K. H. *E. J. Inorg. Chem.* **2012**, 520−529. (b) Zhou, W.; Chiang, L.; Patrick, B. O.; Storr, T.; Smith, K. M. *Dalton Trans.* **2012**, accepted for publication, DOI: 10.1039/C2DT30160A.
(45) Ackermann, M. N.; Barton, C. R.; Deodene, C. J.; Specht, E. M.; Keill, S. C.; Schreiber, W. E.; Kim, H. *Inorg. Chem.* **1989**, *28*, 397−403.
(46) (a) Joy, S.; Krämer, T.; Paul, N. D.; Banerjee, P.; McGrady, J. E.; Goswami, S. *Inorg. Chem.* **2011**, *50*, 9993−10004. (b) Sanyal, A.; Chatterjee, S.; Castiñeiras, A.; Sarkar, B.; Singh, P.; Fiedler, J.; Záliš, S.; Kaim, W.; Goswami, S. *Inorg. Chem.* **2007**, *46*, 8584−8593.
(47) Meredith, M. B.; Crisp, J. A.; Brady, E. D.; Hanusa, T. P.; Yee, G. T.; Pink, M.; Brennessel, W. W.; Young, V. G. *Organometallics* **2008**, *27*, 5464−5473.
(48) Cramer, C. J. *Essentials of Computational Chemistry: Theories and Models*, 2nd ed.; John Wiley & Sons Ltd: West Sussex, U.K., 2004; pp 279−280.
(49) Hagen, K.S., unpublished results. This compound was prepared analogously to $Fe(OTf)_2{\cdot}2MeCN$ (Hagen, K. S. *Inorg. Chem.* **2000**, *39*, 5867−5869) in aqueous triflic acid.